The role of Sterol 12α- hydroxylase (*Cyp8b1*) in Glucose Homeostasis

by

Achint Kaur

B. Tech, VIT University, 2011

A THESIS SUBMITTED IN PARTIAL FULFILLMENT OF

THE REQUIREMENTS FOR THE DEGREE OF

MASTER OF SCIENCE

in

THE FACULTY OF GRADUATE AND POSTDOCTORAL STUDIES

(Medical Genetics)

THE UNIVERSITY OF BRITISH COLUMBIA

(Vancouver)

April 2014

Abstract

Besides their role in facilitating lipid absorption, bile acids are increasingly being recognized as signaling molecules that activate cell-signaling receptors. Targeted disruption of cytochrome P450 sterol 12α- hydroxylase (*Cyp8b1*) results in complete absence of cholic acid and its derivatives. The impact of *Cyp8b1* deletion has predominantly been studied with respect to development of atherosclerosis and lipid and bile acid metabolism. Here, for the first time, we investigate the impact of *Cyp8b1* deletion on glucose homeostasis. Absence of Cyp8b1 results in improved glucose tolerance, enhanced insulin sensitivity and improved β-cell function in *Cyp8b1*$^{-/-}$ mice. In addition, our results show that reduced intestinal fat absorption in the absence of biliary cholic acid in *Cyp8b1*$^{-/-}$ mice leads to increase in free fatty acids reaching the ileal L-cells. This increase in the luminal free fatty acids correlated with significantly increased secretion of the incretin hormone, glucagon like peptide-1 (GLP-1). GLP-1 in turn increases the biosynthesis and secretion of insulin from β-cells, leading to the improved glucose tolerance observed in the *Cyp8b1*$^{-/-}$ mice. Treatment of *Cyp8b1*$^{-/-}$ mice with Exendin (9-39) amide, a potent and selective GLP-1 receptor antagonist, restored their glucose tolerance to control levels. Furthermore, cholic acid feeding in *Cyp8b1*$^{-/-}$ mice resulted in complete normalization of not only fat and glucose tolerance, but also GLP-1 secretion. These data suggest that the absence of cholic acid leads to the improvement in the glycemic control of *Cyp8b1*$^{-/-}$ mice. Thus, our data demonstrates the importance of *Cyp8b1* inhibition in the regulation of glucose metabolism.

Preface

All the experiments in the current study were performed and analyzed by me. J.V. Patankar and W. de Haan helped in performing oral gavages. J.V. Patankar also helped in the design and execution of the luminal fat measurement, exendin (9-39) and bile acid treatment experiments. The bile acid pool measurements were done in collaboration with A. K. Groen at the University Medical Center Groningen, Groningen. P. Ruddle and I performed the genotyping of mice. All the animal work in this thesis was approved by the UBC Animal Care Committee (Animal Care Certificate: A12-0149).

A version of Chapter 3 is being drafted as a manuscript:

Kaur A*, Patankar JV*, de Haan W, Ruddle P, Wijesekara N, Groen AK, Verchere CB, Singaraja RR and Hayden MR (2014) Loss of *Cyp8b1* improves glucose homeostasis by increasing GLP-1. (*co-first authors)

Table of Contents

List of Tables

List of Figures

List of Abbreviations

BAS	Bile acid sequestrant
CA	Cholic acid
CDCA	Chenodeoxycholic acid
FFA	Free fatty acid
FXR	Farnesoid X receptor
GIP	Glucose dependent- insulinotropic peptide
GLP-1	Glucagon like peptide-1
G6Pase	Glucose-6-phosphatase
HDL	High density lipoprotein
MCA	Muricholic acid
PEPCK	Phosphoenolpyruvate carboxykinase
TC	Total cholesterol
TG	Triglycerides

Acknowledgements

At the outset, I wish to place on record, my sincere thanks and profound gratitude to my supervisor Dr. Michael R. Hayden, who reposed his faith in me and let me undertake this challenging assignment. His ideas have borne fruit and have helped in the successful completion of this project.

I humbly express my sincere thanks to Dr. Roshni R. Singaraja, my mentor, for her constant encouragement and invaluable guidance at different stages of this research work. The way she cares for her students cannot be expressed in words.

I would also like to thank Dr. C. Bruce Verchere and Dr. Colin Ross, my committee members for their essential scientific suggestions and guidance throughout the course of my study.

I greatly appreciate the assistance of Jay for helping me develop this project and for his healthy scientific discussion. I would also like to thank Nadeeja for her unconditional support, Willeke for well-intended criticism and Piers for his ever-entertaining music.

My parents and brother deserve special thanks for always encouraging me to chase my dreams. I have reached this important step in my life only because of the love and support of my family and friends. I would specially like to thank my aunt, Vicky Ahuja and her family in Vancouver for making my stay in this beautiful city, a memorable one.

Dedication

To my grandfather…For I am, who I am because of his blessings…

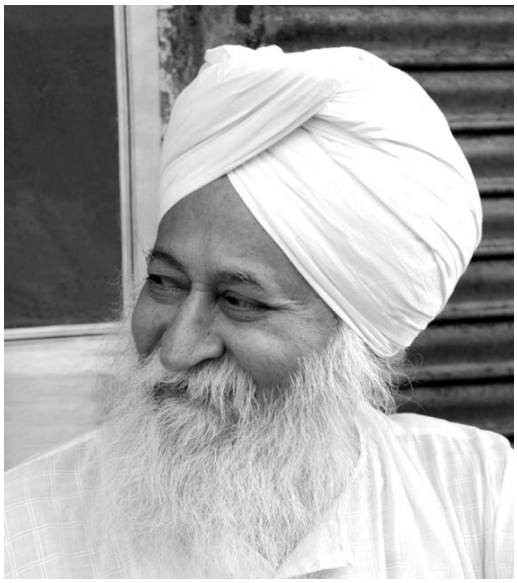

Chapter 1: Introduction

1.1 Overview of glucose metabolism

Glucose is the main type of sugar in the blood and is an important source of energy for all cells in the body. Under physiological conditions, fasting plasma glucose is tightly maintained within the narrow range of 4.4 to 6.1 mM (79.2 to 110 mg/dl) in normal individuals (1). Such tight control of the glucose concentration depends upon both the rate of glucose entering the circulation (glucose appearance) and that of glucose leaving the circulation (glucose disappearance). Glucose appearance in the blood stream is governed by the absorption of glucose from the intestine during the fed state and from hepatic processes like glycogenolysis and gluconeogenesis during the fasted state (1). Glycogenolysis is the breakdown of glycogen, the major storage form of glucose, while gluconeogenesis is the process of generating glucose from other metabolites, primarily lactate and amino acids. On the other hand, glucose disappearance is initiated by the uptake and metabolism of glucose by the peripheral tissues.

1.1.1 Insulin and glucagon

The inability of the body to maintain blood glucose levels within its normal range results in high (hyperglycemia) or low (hypoglycemia) blood glucose. Either of these abnormal conditions can severely interfere with the physiological function of the body. Thus, blood glucose is maintained by the action of two major hormones: insulin and glucagon. Both insulin and glucagon act in a reciprocal manner. Insulin is secreted when the blood glucose concentration rises (>3.3 mM) and it acts by binding to specific insulin receptors on different tissues, like the liver, intestine, muscles and fat, to stimulate glucose uptake (1)(Figure 1.1). On

the other hand, glucagon plays a major role in sustaining the plasma glucose levels during fasting conditions or when the blood glucose concentration falls. Glucagon acts by stimulating hepatic glycogenolysis or gluconeogenesis, thereby counteracting the function of insulin (Figure 1.1). Insulin also inhibits hepatic glucose production and suppresses postprandial glucagon secretion. Insulin and glucagon are secreted by β and α cells of the islets of Langerhans in the pancreas, respectively. Insulin resistance or deficiency results in dysregulation of glucose, thereby increasing fasting and postprandial glucose levels.

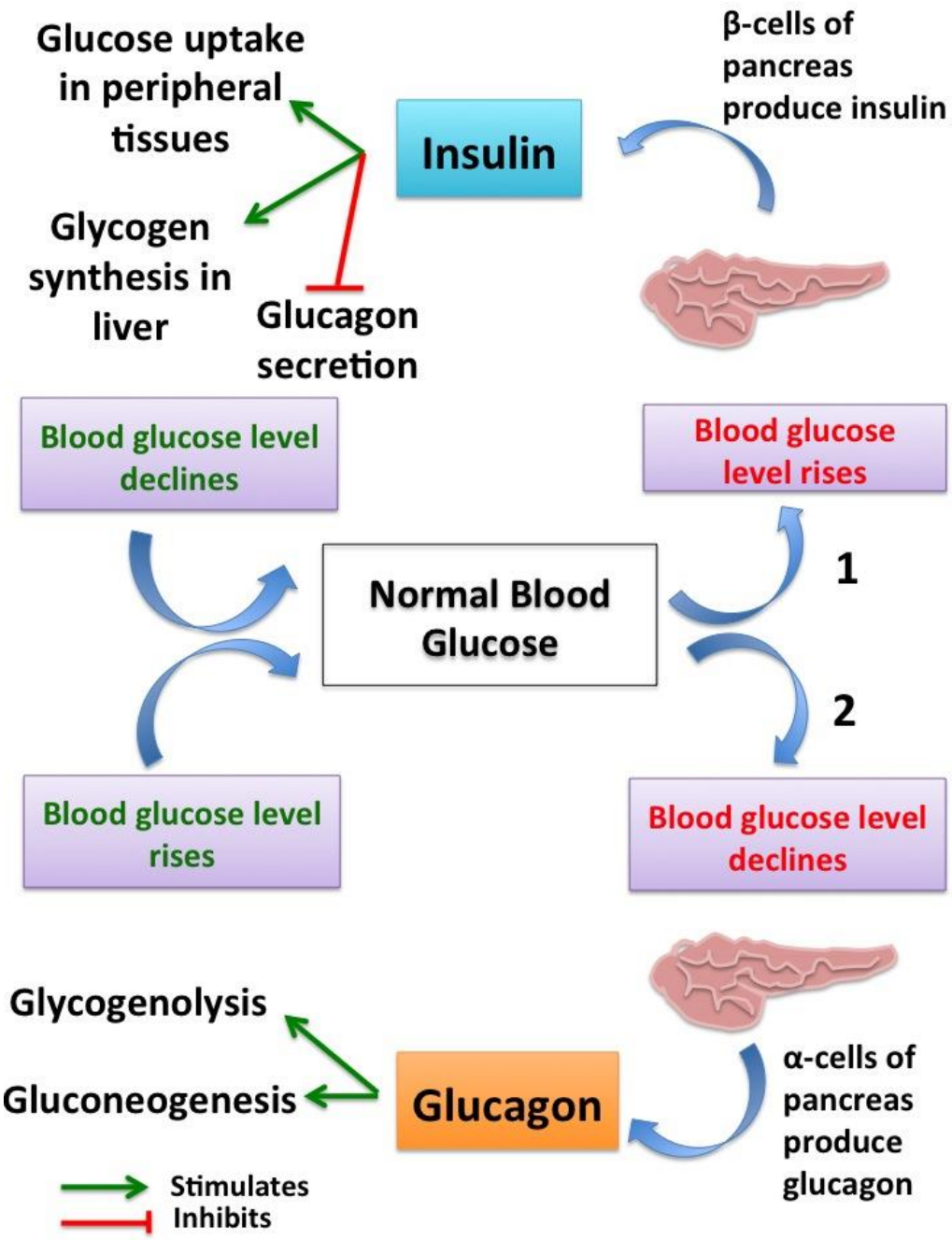

Figure 1.1 Glucose homeostasis: roles of insulin and glucagon

1. Rise in blood glucose causes the release of insulin from the pancreatic β-cells. Insulin, in turn, promotes glucose uptake in cells and storage as glycogen in the liver.
2. Fall in the blood glucose stimulates pancreatic α-cells to release glucagon, which causes the liver to breakdown glycogen and release glucose

1.1.2 Insulin actions

The primary action of insulin is to stimulate glucose uptake into cells. Insulin, therefore, helps to maintain postprandial glucose homeostasis in three ways:

1. Increases peripheral glucose uptake: Insulin signals the cells of insulin sensitive peripheral tissues like the skeletal muscles and adipose tissues to take up and store glucose, until further required. This glucose uptake is facilitated by the action of key signaling molecules such as Protein kinase B (Akt) and phosphoinositide-3 kinase (PI3K) and glucose transporter 4 (GLUT4) (2).
2. Increase in hepatic glycogenesis: Insulin stimulates the liver to store glucose in the form of glycogen (3).
3. Inhibits glucagon secretion: Insulin inhibits glucagon secretion from the pancreatic α-cells, thereby signaling the liver to stop glucose production via glycogenolysis and gluconeogenesis (4).

In addition to these glucose-lowering actions, insulin also exerts other direct and indirect actions on other tissues (5)(Figure 1.2). These include:

1. Increased lipid synthesis: Insulin promotes fatty acid synthesis in the liver. This happens when liver is saturated with glycogen, and any additional glucose that is taken up by the hepatocytes results in the synthesis of fatty acids (6).
2. Decreased lipolysis: Insulin inhibits the breakdown of fats in the adipose tissue by inhibiting intracellular lipase, which breaks down triglycerides into fatty acids (6).
3. Increased amino acid uptake: Insulin stimulates the cells to absorb circulating amino acids.

4. Increased protein synthesis: Insulin stimulates protein synthesis in muscles by activating different components of the translational machinery.
5. Decreased proteolysis: Insulin also inhibits the breakdown of protein
6. Increases uptake of ions: Insulin increases the permeability of many cells to potassium, magnesium and phosphate ions.
7. Decreases appetite: Insulin reduces food intake through hypothalamic regulation in the brain. It also enhances learning and memory and benefits verbal memory in particular.

All the above-mentioned actions of insulin rebalance the blood glucose concentration.

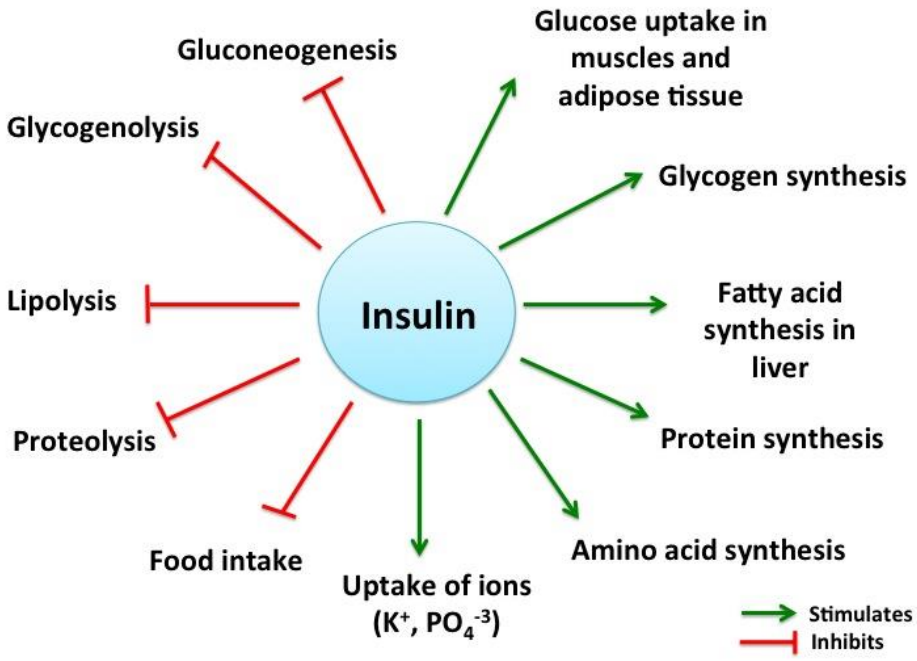

Figure 1.2 Physiological actions of insulin

1.1.3 Glucose stimulated insulin secretion

The process by which insulin is released from the β-cells in response to elevated blood glucose has been well studied. First the entry of glucose into the β-cells is facilitated by the type 2 glucose transporter (GLUT2). Once inside, glucose is immediately phosphorylated by glucokinase to produce glucose-6-phosphate, which is the key metabolite in glycolysis. Glycolysis in the essential energy producing process in the cell, where glucose-6-phosphatae is metabolized to form pyruvate in multiple steps. These glycolytic reactions are accompanied by the production of ATP, the central energy molecule of the cell. Following the increase in ATP levels, the ATP:ADP ratio inside the cell increases and causes the ATP-gated potassium (K_{ATP}) channels to close. This prevents the positively charged potassium ions from exiting the β-cells, immediately resulting in the depolarization of the cell membrane. The net effect is the activation of the voltage-gated calcium channels, which transports calcium into the cells. The resulting drastic increase in the cytosolic concentration of the calcium ions potentiates the exocytosis of insulin from the pancreatic β-cells (Figure 1.3) (7,8).

Insulin release is a biphasic process. The initial amount of insulin released upon glucose absorption is dependent on the amount of insulin available in storage. Once depleted, a second phase of insulin release is initiated. The second phase of insulin release involves the synthesis, processing, and secretion of insulin in response to increase in blood glucose. Once secreted, insulin molecules circulate throughout the blood stream until they bind to their receptors in different tissues, where they exert their glucoregulatory actions (8,9).

Although insulin is undoubtedly one of the most important players in regulating glucose metabolism, another class of hormones called the 'incretins', have emerged as key contributors to the maintenance of glucose homeostasis.

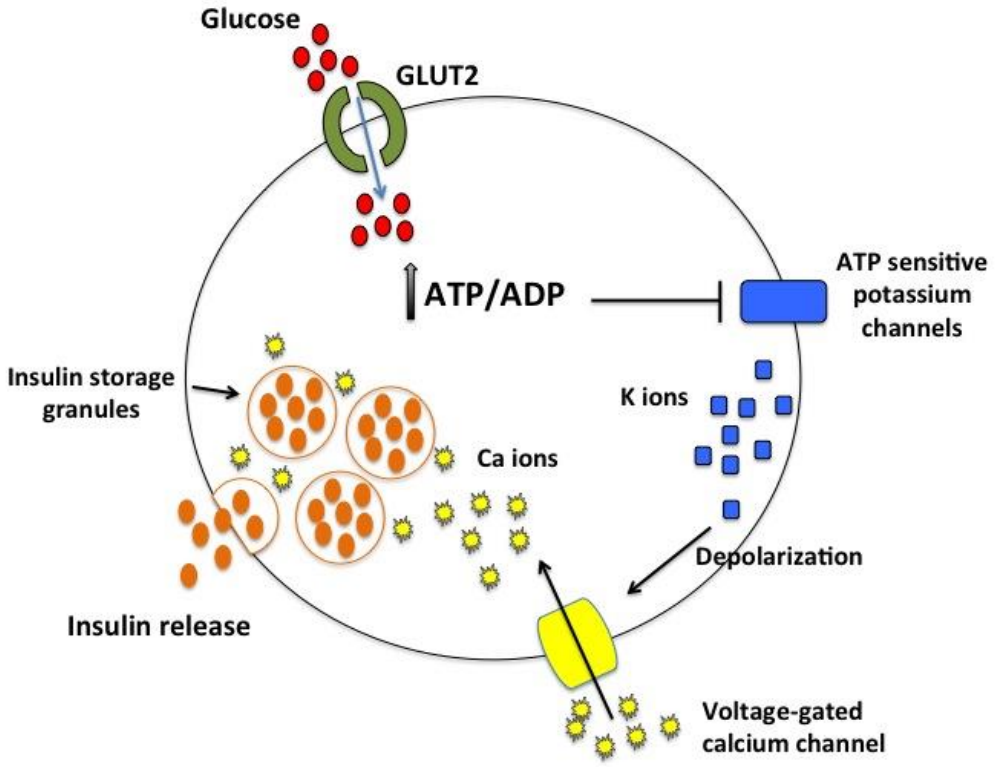

Figure 1.3 Key steps leading to glucose-stimulated insulin secretion
Increased levels of blood glucose trigger its uptake into the β-cells via the GLUT2 transporter. The glycolytic phosphorylation of glucose causes increased ATP: ADP ratio, which inactivates potassium channels. Resulting membrane depolarization opens calcium channels and the influx of calcium causes exocytotic release of insulin.

1.1.4 Incretin hormones

Similar to insulin, incretins are hormones released into the blood stream following meal ingestion. These hormones are however, derived and secreted from the gut. They are produced in

the intestinal mucosa and interestingly are capable of stimulating the release of insulin from the pancreas (10). In the 1960's, studies by three independent groups showed that an oral glucose bolus elicits greater insulin response compared to an intravenous glucose infusion of the same amount of glucose. This phenomenon was referred to as the 'incretin effect' and accounts for almost 50-70% of the total insulin secreted after oral glucose ingestion (11). Until now, only two hormones fulfill the definition of incretin hormones in humans. They are glucose dependent-insulinotropic peptide (GIP) and glucagon like peptide-1 (GLP-1).

1.1.4.1 GIP

GIP, a 42-amino acid peptide, was the first incretin hormone to be identified. It is derived from the differential processing of a 153 amino acid precursor encoded by the *GIP* gene. GIP was formally called gastric inhibitory peptide, due to its role in inhibiting gastric acid secretion and gastrointestinal motility in dogs (11). GIP is synthesized and released from the enteroendocrine K-cells, present mostly in the upper intestinal tract (duodenum and proximal jejunum) in response to glucose or fat ingestion.

In addition to being insulinotropic, GIP is involved in fat metabolism in adipocytes and promotes β-cell proliferation. The presence of GIP in the blood stream is temporary, as it has a very short life due to rapid degradation by the action of the proteolytic enzyme dipeptidyl peptidase-4 (DPP-4) (11).

However, immunoneutralization of GIP only diminished and did not completely abolish the incretin effect observed in rodents, suggesting the presence of another incretin hormone, which was later found to be GLP-1 (12).

1.1.4.2 GLP-1

Glucagon like peptide-1 (GLP-1) was the second incretin to be discovered following the cloning and characterization of the human *proglucagon* gene. The *proglucagon* gene encodes not only glucagon, but also GLP-1, GLP-2 and other proglucagon derived peptides. GLP-1 is produced by post-translational cleavage of *proglucagon* by the prohormone convertase PC1/3 (11).

Although both GLP-1 and GLP-2 are secreted from the enteroendocrine L-cells predominantly present in the distal intestine (ileum and colon), only GLP-1 has insulinotropic properties. GLP-1 is secreted in response to nutrient ingestion. The fasting plasma levels of bioactive GLP-1 in humans increase approximately 2- to 3-fold post a meal. Different nutrients including glucose and other sugars, fatty acids and dietary fibers, are all capable of stimulating the L cells to release GLP-1 (12). In addition to nutrient-mediated release, there is also evidence that GLP-1 release is indirectly controlled by neural and endocrine factors. In particular, the vagus nerve has been shown to mediate GLP-1 release in rats. GIP-induced GLP-1 secretion *in vitro* in canine L-cells and *in vivo* in rodents has also been established (13,14).

Furthermore like GIP, the bioactive GLP-1 is rapidly degraded by DPP-4, and has a half-life of less than 2 minutes in the circulation (12).

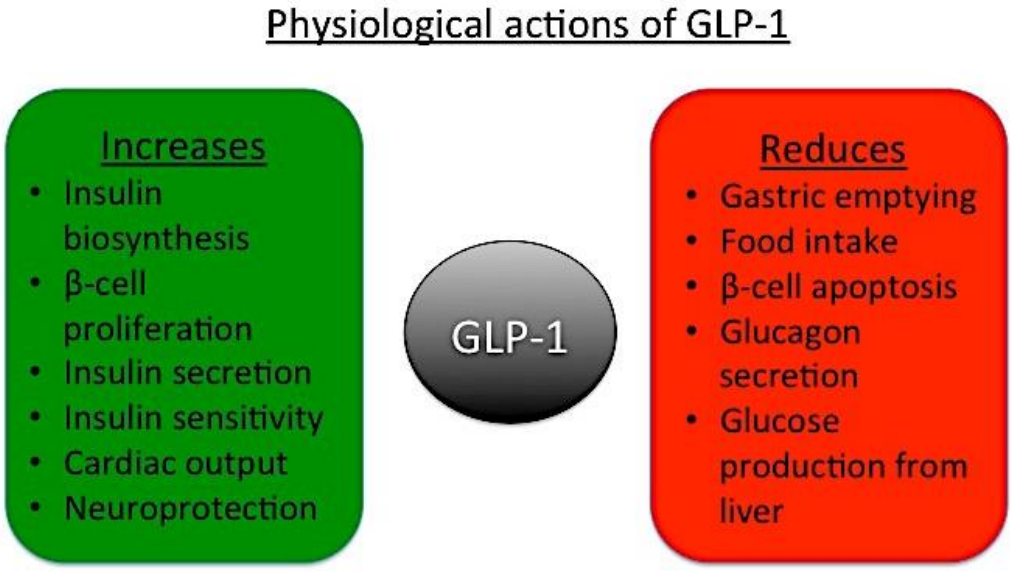

Figure 1.4 Physiological actions of GLP-1 in the peripheral tissues

How does GLP-1 induce insulin secretion? Upon binding to the GLP-1 receptor present on the pancreatic β-cells, GLP-1 triggers a cascade of downstream signaling pathways, which results in increased intracellular cAMP and Ca^{2+} levels in the β-cells. As mentioned previously, increased intracellular Ca^{2+} levels stimulate insulin exocytosis from the β-cells. In addition to the stimulation of glucose-dependent insulin secretion, GLP-1 inhibits gastric emptying, reduces food intake and inhibits glucagon secretion. Together, these beneficial effects of GLP-1 have resulted in the development of new anti-diabetic drugs mimicking GLP-1. These drugs have been shown to alleviate hyperglycemia in type-2 diabetes (T2D) patients (11) (Figure 1.4). Furthermore, development of strategies to increase endogenous GLP-1 could have potential therapeutic application in T2D.

1.2 Diabetes mellitus

Diabetes mellitus is a disease condition where either the pancreas can no longer produce enough insulin, or the body stops responding to the insulin that is produced, resulting in hyperglycemia.

There are two common forms of diabetes. Type 1 diabetes (T1D) is characterized by autoimmune destruction of pancreatic β-cells. Type 2 diabetes (T2D), on the other hand, is caused by a combination of insulin resistance, the inability of the body to achieve adequate insulin secretory response and excessive or inappropriate glucagon secretion (1). T2D is often regarded as a component of the metabolic syndrome, which is characterized by obesity, elevated blood pressure, elevated fasting glucose, increased serum triglycerides and insulin resistance. The prevalence of both T2D and the metabolic syndrome is reaching epidemic proportions. Furthermore, the average age of onset of both these diseases has markedly decreased over the past few decades. Over 380 million children and adults were affected with diabetes in 2013. This number is expected to rise to 592 million by 2035 (http://www.idf.org/diabetesatlas). T2D is also the most prevalent form of diabetes, representing over 90% of all diabetics worldwide. Canadian guidelines define three groups based on their fasting blood glucose: normal (< 6.1 mM), pre-diabetic (6.1-6.9 mM) and diabetic (> 7.1 mM) (http://www.diabetes-blood-sugar-solutions.com/).

In insulin resistance, the production of insulin is (initially) normal, but the insulin response induced in the target peripheral tissues is blunted. Furthermore, insulin resistance results in increased free fatty acids in the circulation, decreased insulin stimulated glucose uptake

and increased gluconeogenesis, resulting in hyperglycemia. In healthy individuals, insulin resistance is overcome by increasing insulin secretion from the pancreatic β-cells, aided by increased β-cell mass or increased insulin biosynthesis. However, in T2D patients, β-cells fail to re-attain optimal insulin secretion. Continued overproduction of insulin from β-cells leads to oxidative and endoplasmic stress and eventual β-cell death, resulting in loss of β-cell mass and β-cell dysfunction, and thus, full onset of T2D (15,16).

Due to the exponential rise in the prevalence of T2D, there is an urgent need to develop improved therapeutic strategies to combat this disorder. Over the past two decades, there has been growing evidence that bile acid metabolism is altered in patients and animal models of diabetes (17). Furthermore, manipulation of the bile acid pool has been shown to improve glycemic control in these patients (18). The underlying molecular mechanisms involved, however, are a subject of ongoing investigation.

1.3 Bile acids

1.3.1 Overview

Bile acids function as powerful detergents to facilitate absorption of lipids and nutrients in the small intestine. They are formed as end products of cholesterol catabolism in the liver. After being synthesized in the hepatocytes, these water-soluble steroids are secreted into the bile canaliculi and then stored in the gall bladder until food ingestion. Upon nutrient intake, the gallbladder releases the bile into the intestine to facilitate digestion. The digestive process is accompanied by the coating of the fats with the bile salts resulting in micelle formation. The

micelles break down the fat molecules into fatty acids and monoglycerides. These breakdown products of fats pass through the epithelial cells of the small intestine eventually forming chylomicrons that enter the lymphatic and then the blood circulation. These bile salts are reabsorbed by both passive diffusion and active transport from the terminal intestine and transported back into the liver, forming the enterohepatic circulation of bile acids (9). More than 95% of the bile salts are re-circulated in this manner, forming a very efficient system to maintain the bile acid pool within the body. The remaining ~5% of the bile acids that do not undergo recycling, go to the colon, where they are excreted in the feces. Such bile acids lost through fecal excretion are replaced by newly synthesized bile acids in the liver (19), thereby maintaining the overall bile acid pool.

Apart from being ‘digestive surfactants’, bile acids are increasingly being recognized as signaling molecules that are specific ligands for the activation of nuclear and membrane receptors. For instance, bile acids act as ligands of nuclear receptors like pregnane X receptor (PXR; NR1I2) and vitamin D receptor (VDR; NR1I1). However, the most well studied bile acid induced signaling pathways involve activation of nuclear receptors like farnesoid X receptor (FXR; NR1H4) and G- protein-coupled receptors (GPCRs) such as TGR5 (GPBAR1, M-BAR and BG37). Through these signaling pathways, bile acids have been shown to regulate cholesterol, glucose and energy homeostasis, in addition to the regulation of their own synthesis (9). Therefore, targeting bile acid controlled signaling pathways can be a promising method to develop novel therapeutics for the management of metabolic syndromes.

1.3.2 Bile acid regulation

Although bile acids are essential for nutrient digestion, these amphipathic molecules are strongly cytotoxic when accumulated in high concentrations. For instance, excessive bile acids can damage cell membranes, cause cholestasis, cirrhosis and hinder liver function (20). Thus, bile acids and their derivatives are readily conjugated with either glycine or taurine in the liver before being transferred into the bile. This conjugation process prevents bile acids from penetrating the cell membranes that line up along the intestinal lumen, thus protecting cells against bile acid cytotoxicity.

Bile acids that are synthesized from the hepatocytes are referred to as primary bile acids. Cholic acid (CA) and chenodeoxycholic acid (CDCA) are the primary bile acids. These primary bile acids are further modified by the gut microbiota into secondary metabolites, referred to as secondary bile acids. The body tightly regulates the bile acid pool. Remarkably, bile acids control their own biosynthesis from cholesterol through an elaborate feedback mechanism governed by interplay of several nuclear receptors.

Firstly, bile acids control their own hepatic synthesis by binding to FXR. FXR is activated by both primary and secondary bile acids, with CDCA being its most potent natural ligand. FXR also acts as a regulator of bile acid synthesis through transcriptional induction of the nuclear receptor, small heterodimer partner (SHP; NR0B2). SHP activation in the liver in turn inhibits the transcriptional activation of *Cyp7a1*, the rate-limiting enzyme for bile acid synthesis. Thus, bile acids regulate their own biosynthesis following the activation of FXR (20,21).

Secondly, in addition to bile acid regulation via hepatic FXR, intestinal FXR is also involved in the regulation of bile acid synthesis. Following a meal, the bile acid influx activates FXR in the intestine, which induces the expression of fibroblast growth factor-19 (FGF-19/FGF-15 in rodents). Fgf15/19 is released by the enterocytes, the epithelial cells of the small intestine, and circulates until it reaches the liver and binds to the cell surface FGF-receptor 4 (Fgfr4). This binding between Fgf15/19 and Fgfr4 signals the reduction in bile acid synthesis via the c-Jun NH2- terminal kinase (JNK) pathway (9).

Furthermore, growing evidence suggests that FXR controls the expression of proteins that are involved in the shuttling of bile acids from the apical to the basolateral sides of the enterocytes on reabsorption. These proteins include the apical sodium-dependent bile acid transporter (ASBT) and the ileal bile acid-binding protein (IBABP). FXR also induces the expression of organic solute transporter α and β heterodimer (OSTα/OST β) located on the basolateral membrane of the enterocytes, which effluxes bile acids into the portal blood circulation. Once in the circulation, bile acids are taken up by Na+ taurocholate co-transporting polypeptide (NTCP), which returns the bile acids to the liver. FXR also inhibits the transcription of NTCP in an SHP-dependent manner. Deficiency in FXR regulation of the enterohepatic circulation of bile acids may result in cholestasis.

In short, FXR plays a critical role in the regulation of *de novo* bile acid synthesis as well as in maintaining their enterohepatic circulation (20).

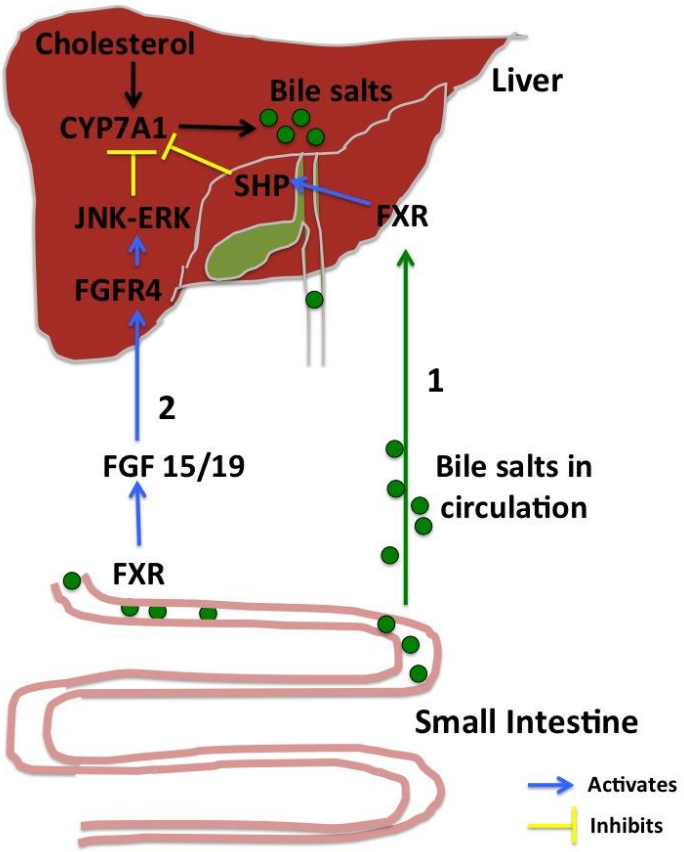

Figure 1.5 FXR mediated regulation of bile acids

1. Hepatic farnesoid X receptor (FXR) is activated by bile acids, which in turn induces the expression of short heterodimer partner (SHP) to inhibit the activity of CYP7A1, the rate-limiting enzyme in the bile acid synthesis.
2. Upon activation by the bile acids, the intestinal FXR induces the expression of fibroblast growth factor (FGF 19/ Fgf 15 in rodents). FGF15/19 binds to the hepatic surface receptor (FGFR4) and activates the downstream JNK-ERK pathway to inhibit the activity of CYP7A1. (Adapted from http://atvb.ahajournals.org/content/30/8/1519/F1.large.jpg)

1.3.4 Bile acids and lipid metabolism

In addition to its role in regulating bile acid synthesis, FXR activation also alters the transcription of several genes involved in triglyceride synthesis and lipid metabolism. Indeed, mice lacking FXR are dyslipidemic with high levels of plasma triglycerides (TG) and non-high density lipoprotein (HDL) cholesterol levels. FXR null mice also have increased synthesis of apo

B-containing lipoproteins, mainly very low-density lipoprotein (VLDL), and increased intestinal cholesterol absorption. On the other hand, activation of FXR using synthetic agonists reduces cholesterol absorption by over 50% (22). Thus, bile acid mediated FXR activation plays a crucial role in maintaining lipid metabolism.

Moreover, bile acids also affect triglyceride homeostasis. The inverse relationship between serum bile acids and serum triglycerides has been well established. FXR activation has been shown to increase triglyceride clearance by inducing the expression of apolipoprotein C-II (apoC-II) and repressing apolipoprotein C-III (apoC-III). ApoC-II and apoC-III are co-activator and inhibitor, respectively, of lipoprotein lipase (LPL), which induces the lowering of serum triglycerides (23). Furthermore, FXR-stimulated SHP inhibits LRH-1 mediated activation of sterol regulatory binding protein-1c (SREBP-1c) expression. SREBP-1c is the main regulator of fatty acid and triglyceride synthesis in the body (9).

Additionally through interaction with TGR5, the other potent bile acid receptor, bile acids also affects hepatic lipid content. Mice lacking TGR5 have increased hepatic fat content and this effect is reversed upon administration of TGR5 agonists (22).

Overall, activation of both the major bile acid receptors (FXR and TGR5) reduces hypertriglyceridemia and hepatic steatosis and thus, plays a major role in maintaining lipid metabolism.

1.3.5 Bile acid and glucose metabolism

In addition to their role in maintaining lipid metabolism, bile acids are increasingly being recognized as regulators of glucose metabolism. This is specially highlighted by the presence of altered bile acid composition and pool in human and animal models of diabetes. For example, a recent study showed that FGF15/19, which are downstream targets of FXR in the intestine, act as postprandial factors that control glycogen synthesis and thus play an important role in maintaining postprandial glucose metabolism (9).

Studies have also shown that FXR plays a crucial role in regulating the gluconeogenic genes, phosphoenolpyruvate carboxykinase (PEPCK) and glucose-6-phosphatase (G6Pase) (23). However, the proposed mechanisms and physiological effects remain controversial. Some studies report that FXR activation increases the expression of PEPCK and glucose output in human hepatocytes, while other studies show that mice deficient of FXR are hyperglycemic and insulin resistant, in contrast to the previous finding. Furthermore, administration of FXR agonists to FXR knockout mice reverses these effects and improves their insulin sensitivity.

There is also evidence that suggests that FXR activation is associated with increased AKT (also known as protein kinase B) phosphorylation and glucose transporter, GLUT2, translocation to the cell membranes. Both these processes collectively are responsible for improving peripheral insulin sensitivity. Together, these data suggest the critical role of FXR activation in modulating glucose homeostasis. However, further and more comprehensive investigation is required to better clarify the remaining ambiguity.

Bile acid sequestrants (BAS), which are resins that form non-absorbable complexes with the bile acids in the intestine and prevent them from being re-absorbed, are increasingly being used for the treatment of patients with diabetes. BAS have classically been used for over 40 years in the treatment of dyslipidemia, however they have also been shown to improve glucose homeostasis in different studies. BAS treatment lowers fasting glucose and improves insulin sensitivity in both men and different experimental models. Several pre-clinical and clinical studies in patients with diabetes mellitus have shown that by altering the bile acid synthesis, bile acids may have effects on both insulin secretion and peripheral insulin sensitivity (17,18). These data suggest that bile acids play a significant role in maintaining glucose metabolism.

An additional role of bile acids in regulating glucose homeostasis is reflected by their involvement in improving energy expenditure in a TGR5-dependent manner. Upon activation with bile acids, TGR5 results in the production of intracellular cAMP. The increase in cAMP concentration activates protein kinase A (PKA), which phosphorylates cAMP response element (CREs) in their promoter. This cascade results in the induction of downstream fatty acid oxidation genes and increases energy expenditure, thereby promoting weight loss. The TGR5 mediated regulation of weight loss could play an important part in maintaining glucose homeostasis (23). In addition to being highly expressed in the liver, the adipose tissue and the spleen, TGR5 is also expressed in the intestine, where it plays a major role in stimulating the release of the incretin hormone, glucagon like peptide-1 (GLP-1). Incretins, as described previously, are hormones that play a crucial role in maintaining glucose metabolism and anti-diabetic drugs based on GLP-1's physiological effects are being used clinically. These findings establish the role of bile acid mediated processes in regulation of glucose homeostasis.

1.3.5.1 Bile acids and GLP-1

GLP-1 secretion *in vivo* is stimulated upon the arrival of nutrients to the L-cells. Bile acids, which are released into the duodenum from the gall bladder after food ingestion, are also present in the intestinal lumen and have been shown to stimulate GLP-1 release.

As previously mentioned, bile acids act as ligands for TGR5 activation. Studies have shown that bile acids activate GLP-1 production in the murine enteroendocrine cell line STC-1, in a TGR5-mediated manner. The same study demonstrated that lithocholic acid and deoxycholic acid, the two major secondary bile acids, concentration-dependently stimulate intracellular cAMP levels, resulting in GLP-1 release (24). This was the first study to elucidate that bile acids induce GLP-1 in a TGR5-dependent manner. A follow-up study showed that the TGR5-deficient mice have impaired glucose tolerance and that administration of the TGR5 agonist INT777 improved GLP-1 release *in vivo.* In contrast mice overexpressing TGR-5 had enhanced plasma GLP-1 accompanied by raised intracellular ATP/ADP ratio and calcium influx (25). These studies establish the important role bile acids play in directly activating GLP-1 release via TGR activation.

For bile acids to activate GLP-1, they should be present in the terminal ileum and the colon, where majority of the TGR5 is expressed. However, Colesevelam, a well-known bile acid sequestrant (BAS), which preferentially binds CA, has been shown to improve glucose tolerance in humans (17). Since BAS diminish the amount of bile acids available to act on the terminal ileum, the direct role of TGR5 in improving glucose homeostasis is unclear. An alternate mechanism for the modulation of GLP-1 by BAS involves increased free fatty acid (FFA)

content in the ileum due to defective micellar solubilization in the jejunum post BAS treatment (26), suggesting that the BAS exert their effects in a bile acid receptor- independent manner. In addition, this mechanism could explain improvements in glycemic control following intestinal transposition or other bariatric surgery.

Therefore, increasing the bile acid pool by either increasing bile acid synthesis or by using BAS could be a potential therapeutic strategy to increase the secretion of GLP-1.

1.4 Bile acid synthesis

Bile acid synthesis is the primary pathway for the catabolism of cholesterol. *De novo* biosynthesis of bile acids takes place exclusively in the liver, as the necessary enzymatic machinery resides only here. The human liver converts approximately 500 mg of cholesterol into bile acids every day (9).

The primary pathway, also referred to as the classical or neutral pathway, is the major bile acid biosynthesis pathway in the liver and accounts for at least 75% of the total bile-acid pool (Figure 1.6). This pathway converts cholesterol to 7α-hydroxycholesterol, followed by a series of enzymatic reactions, eventually producing the primary bile acids, i.e. cholic acid (CA) and chenodeoxycholic acid (CDCA). The classical pathway involves the action of the cytochrome P450 enzymes, cholesterol 7α-hydroxylase (*CYP7A1*) and sterol 12α- hydroxylase (*CYP8B1*). Both these enzymes are present in the membrane of the endoplasmic reticulum. Importantly, CYP7A1 is the first and the rate-limiting enzyme of the classical pathway. As such, mice lacking *Cyp7a1* have severely impaired bile acid synthesis and subsequently suffer from

defective absorption of lipids and vitamins which results in perinatal mortality (27,28). Additionally, homozygous deletion mutations in the human *CYP7A1* gene have been correlated with increased risk of hypercholesterolemia and atherosclerosis (29). The reactions downstream of *CYP7A1* in the classical pathway are catalyzed by CYP8B1. *CYP8B1* is responsible for the production of CA and is crucial for maintaining the CA/CDCA ratio in the bile. The ratio of CA to CDCA is an important determinant for the solubility of bile cholesterol and the absorption of cholesterol from the intestine. If not maintained to optimal levels, the CA/CDCA ratio may influence gall stone formation in the gall bladder and also result in hypercholesterolemia (30,31).

Besides the classical pathway, mammals also have another pathway, known to as the alternate or the acidic pathway (Figure 1.6). The alternate pathway involves the action of 27-hydroxylase (*CYP27A1*), followed by a series of reactions, ending in the production of CDCA. The alternate pathway facilitates the removal of excessive cholesterol from the peripheral tissues (32). It is hypothesized that *CYP27A1* present in the peripheral tissues converts cholesterol into oxysterols, which are more water-soluble than cholesterol. These metabolites and then transported to the liver where they are converted into bile acids. It is for this reason that the alternate pathway has been proposed to be important in reverse cholesterol transport (19,33).

The bile acid pool in humans consists of predominantly hydrophobic bile acids, like CD A, CA and DCA. On the contrary, mice have mostly hydrophilic bile acids, like muricholic acids (MCA) and CA, because mice readily convert CDCA to MCA in their livers (34).

A fraction of CA and CDCA is converted into their secondary bile acids, deoxycholic acid (DCA) and lithocholic acid (CDCA) respectively by the action of bacteria, when the bile acids reach the colon (9).

1.5 *Cyp8b1*

1.5.1 Structure, function and regulation

Sterol 12α- hydroxylase (CYP8B1) is a cytochrome P-450 enzyme, exclusively present in the liver. Ishida et al. in 1992 were the first group to purify CYP8B1 from rabbit liver microsomes (35). The human and mouse CYP8B1 genes were cloned and characterized by Gafvel et al in 1998. This gene is highly conserved within mammals. Human *CYP8B1* is located on chromosome 3p21.3-22 and is 3,950 bp in length. The murine counterpart is approximately 3kb long and located on chromosome 9qF4, a region homologous to human chromosome 3. Furthermore, *CYP8B1* is intron-less. The mouse and human *CYP8B1* promoter have ~21% homology and thus different transcriptional regulation. The transcription of the mouse and human *CYP8B1* is initiated from positions 51 and 35 bases, respectively, downstream of the TATA box (36).

As stated previously, the function of *CYP8B1* is to convert of 7α-hydroxyl-4-cholesten-3-one into 7α, 12α-dihydroxy-4-cholesten-3-one, in the classical bile acid synthesis pathway. *CYP8B1* is crucial for the synthesis of CA in the bile. Furthermore, activity of *CYP8B1* determines the ratio of CA to CDCA formed in the classical pathway.

Cyp8b1 gene expression is induced by fasting/starvation. Treatment of mice with peroxisome proliferator agonist or fasting, both increased *Cyp8b1* expression in mice. Insulin also acts as a dominant suppressor of *Cyp8b1* gene expression, as seen in streptozotocin- induced diabeteic mice (37). Sterol regulatory element binding proteins (SREBP) also regulate *Cyp8b1*. While SREBP-1a and -1c enhances the transcription of the *Cyp8b1* gene, SREBP-2 is reported to suppress its promoter activity. In addition, bile acids themselves negatively regulate *Cyp8b1* gene expression, similar to the regulation of *Cyp7a1*, in an FXR-SHP dependent manner (37).

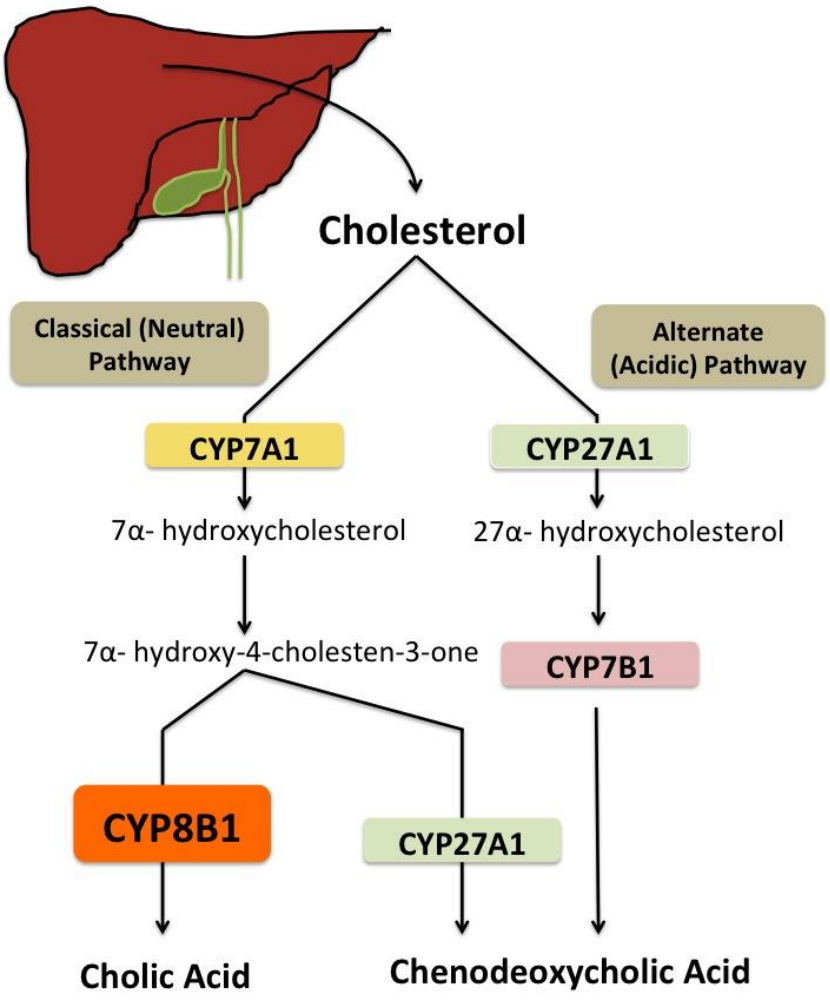

Figure 1.6 Bile-acid synthesis pathways
Cholesterol is converted into bile acids via two major pathways: The classical (or neutral pathways) pathway and the alternate (or acidic) pathway. Only major enzymes and their substrates and metabolites are shown.

1.5.2 *Cyp8b1* knockout mouse model

The activity of *Cyp8b1* is crucial for the production of CA. Hence, the disruption of *Cyp8b1* in mice results in the complete absence of CA and its metabolites. Lack of CA is compensated by a relative increase in muricholates and CDCA. Li-Hawkins et al. in 2002 were the first group to generate and characterize the *Cyp8b1* knockout (*Cyp8b1*$^{-/-}$) mice (38). *Cyp8b1*$^{-/-}$ mice have an enlarged bile acid pool as a consequence of the up-regulation of *Cyp7a1* (38). The resulting increase in hydrophilic bile acids leads to a reduction in both intestinal absorption and hepatic accumulation of cholesterol (39,40). Addition of cholate restores the intestinal cholesterol absorption and normalizes the *Cyp7a1* activity in *Cyp8b1*-null mice, suggesting the crucial role of CA in regulating lipid homeostasis (40).

The absence of CA synthesis was also studied in apolipoprotein E knockout (*ApoE*$^{-/-}$) mice, a common animal model of atherosclerosis. *Cyp8b1*$^{-/-}$ x *ApoE*$^{-/-}$ mice show 50% reduced atherosclerotic plaques after 5 months of cholesterol feeding compared to *ApoE*$^{-/-}$ mice (41). This effect was associated with reduced intestinal cholesterol absorption, decreased levels of ApoB-containing lipoproteins in the plasma, reduced hepatic cholesteryl esters and enhanced BA synthesis (41).

Furthermore, the role of CA in the development of hypercholesterolemia and gallstones was studied utilizing cholesterol-fed alloxan-induced type 1 diabetic *Cyp8b1*$^{-/-}$ mice (42). Diabetic cholesterol-fed *Cyp8b1*$^{+/+}$ mice had significantly higher biliary cholesterol, cholesterol saturation index and increased cholesterol crystals in their bile compared to the knockout counterparts. Thus, *Cyp8b1*$^{-/-}$ mice are protected against hypercholesterolemia and gall stones

(42). These findings suggest that the absence of Cyp8b1 may be beneficial in cases of metabolic syndrome.

1.5.3 CYP8B1 human genetics

In humans, the two primary bile acids- CA and CDCA are produced in a molar concentration of ~2:1 (43). The loss of the activity of CYP8B1 would lead to the production of CDCA over CA, thereby modifying the bile acid pool and changing the cholesterol absorption. However, differences in the ratio of CA and CDCA in humans cannot be explained by polymorphisms in human *CYP8B1* (30) as of yet. Screening for genetic polymorphism in this study was performed in a 2.4 kb long region including the exon and part of the promoter but no polymorphisms were found in this region (30). To date, there is no published data showing polymorphisms in *CYP8B1* being associated with any disease, since no polymorphisms have been described.

1.6 Research objectives

There have been many studies focusing on the role of CA in the regulation of bile acid and cholesterol synthesis. However, its role in maintaining glucose metabolism is not well elucidated. *Cyp8b1*$^{-/-}$ mice lacking the ability to synthesize CA *in vivo* provide a unique opportunity to more selectively study the contribution of CA in altering glucose homeostasis. Thus, our goal in the present study was to determine the role of *Cyp8b1* in glucose homeostasis.

1.7 Rationale for hypothesis

The main role of bile acids is to facilitate nutrient digestion. The primary bile acids like CA and CDCA, along with their derivatives are released into the small intestine upon food ingestion. The amphipathic bile salts attach to the fat globules forming micelles, which breaks down the fat molecules into fatty acids and monoglycerides. These breakdown products of fats pass through the epithelial cells of the small intestine eventually forming chylomicrons that enter the lymphatic and blood circulation. The fats that are not absorbed in the duodenum and the jejunum further travel to the distal intestine where they activate the L-cells and trigger the release of the incretin, GLP-1 (13).

In *Cyp8b1*$^{-/-}$ mice, the normal digestion process may be disrupted due to the change in the bile acid composition and pool size. We hypothesize that the absence of cholic acid would result in defective micellar solublization of fats, thereby increasing the concentration of free fatty acids reaching the terminal ileum and the colon. More free fatty acids would have a greater activation of L-cells, thus resulting in greater GLP-1 secretion.

Moreover, *Cyp8b1*$^{-/-}$ mice have higher CDCA and its secondary bile acids- lithocholic acid (LCA) levels. LCA potently activates TGR5, thereby resulting in GLP-1 release (24). This suggests that *Cyp8b1*$^{-/-}$ mice may have greater TGR5 activation and thus enhanced GLP-1 release. Additionally, *Cyp8b1*$^{-/-}$ mice have increased *Cyp7a1* gene expression and it has been shown that mice overexpressing *Cyp7a1* are protected from high-fat induced insulin resistance (44). Collectively, these studies suggest that inhibition of *Cyp8b1* may improve glucose homeostasis in mice.

1.8 Hypothesis

We hypothesized that knockout of *Cyp8b1* will enhance insulin sensitivity, increase insulin secretion and improve glucose homeostasis in mice via the activation of GLP-1.

1.9 Research plan

A mouse model with targeted deletion of the *Cyp8b1* gene was utilized for this study. Both male and female mice were characterized at 3 and 6 months of age on a chow diet, or following 4-6 weeks on a high cholesterol diet. The use of a 0.5% cholesterol diet has previously been shown to increase HDL cholesterol levels in *Cyp8b1*$^{-/-}$ mice (40). Plasma total cholesterol, HDL cholesterol and plasma triglycerides were measured, to confirm the phenotype of *Cyp8b1*$^{-/-}$ mice. Fasting plasma blood glucose and fasting plasma insulin, glucose tolerance, insulin tolerance and fat tolerance were determined. GLP-1 levels in the plasma of these mice 30 minutes post glucose gavage were determined. *In vivo* glucose stimulated insulin secretion, insulin content in isolated islets, and β-cell mass were also measured. We also measured the circulating bile acid pool of *Cyp8b1*$^{-/-}$ mice. Bile acid pool measurements were performed in collaboration with Dr. A. K. Groen at the University Medical Center Groningen, Groningen. Finally GLP-1 receptor antagonist experiments and rescue experiments with CA were performed.

The results presented here are of 3-month-old female mice on chow and following 4-6 weeks on 0.5% cholesterol diet (HCD) (as indicated). The 6-month-old female mice on chow and HCD showed similar phenotype as the 3-month-old female mice, hence, those data are presented in Appendix B. Male mice showed no changes in the metabolic parameters analyzed at both 3 and 6 months on both chow and HCD (Appendix C-E).

Chapter 2: Materials and Methods

2.1 Animals and diet

Cyp8b1$^{+/-}$ mice were purchased from UC Davis KOMP repository (*Cyp8b1*$^{tm1(KOMP)Vlcg}$). Control and *Cyp8b1*$^{-/-}$ mice were obtained by breeding *Cyp8b1*$^{+/-}$ mice. Genotyping was performed on genomic DNA extracted from tail snips, according to the manufacturer's protocol (Kapa Biosystems). Regular PCR was performed using the forward and reverse primers I and III for control mice and primers II and IV for *Cyp8b1*$^{-/-}$ mice.

Primer	**Sequence**
I	CCAGCTCCTGGTGTGAAGATGG
II	TGGGAAATTAACAGTCGCACACATGG
III	GTCCTGCATGGATGAAGCTATTCC
IV	GCAGCCTCTGTTCCACATACACTTCA

Table 1 List of primers used for genotyping

Male and female mice aged 3-6 months were used for this study. Mice had *ad libitum* access to water and standard laboratory chow (Lab Diet), or 0.5% Cholesterol diet (HCD) (Harlan Diets) for 4 weeks. For experiments involving fasting, mice were fasted for 4 hours (7-11am) prior to the procedure. Blood for all experiments was drawn from the medial saphenous vein. Tissue harvesting and islet isolations were performed after 6-8 weeks on HCD.

All experiments were approved by the University of British Columbia Animal Care Committee.

2.2 Biochemical analysis

Blood from fasted mice was drawn from the medial saphenous vein in EDTA coated capillary tubes. Plasma was isolated by centrifugation of the blood containing capillary tube, at 6000 rpm for 10 min at 4^{o} C. Fasting plasma total cholesterol, HDL cholesterol and triglycerides were measured from 5 μL of freshly isolated plasma according to the manufacturer's protocol (Thermo Scientific; Roche).

2.3 Oral fat tolerance testing

Blood was drawn from fasted mice before (0 h) and at time point 2, 4 and 6 h after intra-gastric gavage of 200 μL corn oil. Plasma triglyceride content was measured using the manufacturer's protocol (Roche). For CA feeding experiments, mice were orally gavaged with 17 mg/kg CA (Sigma) or vehicle (1.5% $NaHCO_3$) as previously described (45) and oral fat tolerance tests were performed 30 min post feeding.

2.4 Luminal free fatty acid quantification

Fasted mice were gavaged with a bolus of high fat meal (Research Diets) in PBS (200 μL of 200 mg/mL) and sacrificed 1 h post-gavage. Sections of the intestine (duodenum, jejunum and ileum) were collected in 0.5M sodium taurocholate (Sigma), vortexed and centrifuged at 3000 rpm for 15 min. Lipids were extracted using Folch extraction method (46). Free fatty acids were measured using an enzymatic colorimetric assay (Roche).

2.5 Glucose and insulin tolerance testing

Oral and intra-peritoneal glucose tolerance tests (GTT) were performed on fasted mice by gavaging or injecting 2 g/kg glucose and measuring glucose using a glucometer (Lifescan) at 0, 15, 30, 60 and 90 min post gavage/injection. Insulin tolerance tests (ITT) were performed by injecting 1 U/kg human recombinant insulin (Novo Nordisk) in the fasted mice, followed by measurement of glucose as in the GTT. For CA feeding experiments, mice were orally gavaged with either 17 mg/kg CA or vehicle (1.5% $NaHCO_3$) as previously described (45), for 3 consecutive days at 6 pm and intraperitoneal (IP) GTT was performed on the following day. For bile acid treatment experiments, mice were intraperitoneally injected with 0.125 mg, 0.028 mg, 4.96 μg and 0.011 mg of α, β, ω-MCA, and UDCA per kg body weight, respectively. These values were calculated based on concentrations of individual circulatory bile acids found in excess in the *Cyp8b1*$^{-/-}$ mice and 3 times the concentration was administered. IPGTT was performed 15 min post-administration.

2.6 HOMA-IR calculation

Homeostatis model assessment of insulin resistance (HOMA-IR) was calculated using the formula HOMA-IR (mmol/L × μU/mL)= fasting glucose (mmol/L) × fasting insulin (μU/mL)/22.5 (47).

2.7 GIP and GLP-1 measurement

Fasted mice were gavaged with 2 g/kg glucose and blood was drawn 30 min post-gavage. Plasma was isolated and total GIP and GLP-1 levels were measured by ELISA using the manufacturer's protocol (Mercodia; MSD). For CA feeding experiments, mice were treated as

mentioned above (GTT and ITT). On the following day blood was isolated 30 min post-glucose-gavage to measure plasma GLP-1.

2.8 Exendin-3 treatment

GTT was performed in mice injected with 167 µg/kg body weight of Exendin (9-39) amide (Ex-3) (Tocris) or vehicle (PBS), 30 min prior to an oral glucose gavage.

2.9 Insulin secretion and islet insulin content measurement

To determine insulin secretion *in vivo*, fasted mice were gavaged with 2 g/kg glucose and plasma insulin was measured at different time points by ELISA (Mercodia). Insulin secretion *in vitro* was performed on hand-picked islets isolated after intraductal collagenase injections as previously described (48) or by differential density centrifugation over Histopaque (Sigma-Aldrich). Ten islets per well were incubated in Kreb's Ringer bicarbonate buffer containing 1.67 or 16.7 mM glucose. After 1 h, the media was removed and the islets were lysed in an acid-alcohol buffer (EtOH:H_2O:HCl::150:47:3). Insulin secretion was normalized to islet DNA content. Lysed islets were diluted 1:2000 and islet insulin content was measured using ELISA (Mercodia).

2.10 Real time PCRs

Total RNA was isolated from tissues using RNA extraction kit (Qiagen). One microgram RNA was used to synthesize cDNA using the Superscript III First-strand synthesis kit (LifeTechnologies). Primer sequences used for measuring gene expression are listed in the table. Quantitative real-time PCR was performed in an ABI Prism 7700 Sequence Detection System,

using SYBR Green PCR Master Mix (Applied Biosystems). *Gapdh* was used as the housekeeping gene.

Gene	Forward Primer	Reverse Primer
Abca1	5'-AGG CAT GGA CCC TAA AGC CCG-3'	5'-GAC ACT GCC AAG GCA CCT GAA CC-3'
Sr-b1	5'-GTT GGT CAC CAT GGG CCA-3'	5'-CGT AGC CCC ACA GGA TCT CA-3'
Srebp-1c	5'-GGA GCC ATG GAT TGC ACA TT-3'	5'-GGC CCG GGA AGT CAC TGT-3'
Cyp7a1	5'-ACG CAC CTC GTG ATC CTC TGG G-3'	5'-GGC TGC TTT CAT TGC TTC AGG GCT-3'
Cyp8b1	5'-ATC GCC TGA AGC CCG TGC AG-3'	5'-AGC TGG GGA GAG GAA GGA GTG C-3'
Cyp27a1	5'-GTT CGG TCT TGC CTG GGT CGG-3'	5'-ACT TCT CCC ATC CCG GGA GCC-3'
G6pase	5'-ACT GTG GGC ATC AAT CTC CT-3'	5'-TGT CCA GGA CCC ACC AAT AC-3'
Pepck	5'-ATC ATC TTT GGT GGC CGT AG-3'	5'-CAT GGC TGC TCC TAC AAA CA-3'
Glp-1	5'-GCC CAA GAT TTT GTG CAG TGG-3'	5'-GTC CCT TCA GCA TGC CTC TC-3'
Tgr5	5'-CTC CTG TTG CCT GCC GTG GG-3'	5'-CGC TCC AGT CGG CGG ATC TC-3'
Gapdh	5'-TGC ACC ACC AAC TGC TTA G-3'	5'-GAT GCA GGG ATG ATG TTC-3'

Table 2 List of primers used for gene expression analysis

2.11 Immunofluorescence

Formalin-fixed, paraffin-embedded sections (5 μm) from three areas of the pancreas of HCD fed *Cyp8b1*$^{-/-}$ and control mice were deparaffinized and rehydrated. Antigen retrieval was performed with Target Retrieval Solution (Dako) in a steamer for 20 min. Sections were blocked

with 2% normal goat serum (Vector Laboratories) for 30 min, then incubated with guinea pig anti-insulin (1:200; Dako) in 0.1% BSA/PBS overnight at 4°C. Alexa 594 goat anti-guinea pig secondary antibody (1:200; Invitrogen) was applied for 1 h at room temperature. Slides were mounted using Vectaschield mounting medium with DAPI (Vector Laboratories) and imaged on BX61 microscope (Olympus). Quantification was performed using Image-Pro (MediaCybernetics). β-cell mass was measured by calculating the percentage of insulin-positive surface area from 6 evenly spaced sections per pancreas. The mean insulin-positive area was then multiplied with the pancreatic wet weight to estimate β-cell mass.

2.12 Plasma bile acid measurements

Plasma samples were prepared for and analyzed by gas chromatography mass spectroscopy (GC-MS), as previously described (49).

2.13 Statistical analysis

All data are presented as mean ± SEM. As noted in figure legends, data were analyzed using unpaired Student's t-test with two-tailed analysis or two-way ANOVA followed by Bonferroni post-hoc test.

Chapter 3: Results

3.1 Effect of CA depletion on plasma lipoproteins

Our knockout mouse model confirms the previously published findings of unchanged fasting plasma levels of total cholesterol (TC), HDL cholesterol (HDLc) and triglycerides (TG) (Table 1) (38). When the mice were fed HCD, they showed significant increase in plasma HDLc levels at both 3 and 6 months of age, while no change was observed in the fasting levels of TC and TG (Table 3).

		3 months			6 months		
		Control	***Cyp8b1*$^{-/-}$**	**p value**	**Control**	***Cyp8b1*$^{-/-}$**	**p value**
Chow	TC (mM)	3.18±0.26	3.47±0.25	0.45	2.52±0.13	2.82±0.11	0.32
	HDLc (mM)	2.83±0.17	3.28±0.09	0.056	1.58±0.20	1.76±0.31	0.90
	TG (mg/mL)	1.01±0.09	1.06±0.04	0.93	0.90±0.07	0.79±0.02	0.17
HCD	TC (mM)	3.39±0.27	3.82±0.17	0.21	2.82±0.09	3.19±0.21	0.11
	HDLc (mM)	2.10±0.20	2.87±0.20	0.02*	1.61±0.21	2.36±0.28	0.04*
	TG (mg/mL)	0.59±0.03	0.26±0.16	0.09	0.53±0.02	0.49±0.01	0.19

Table 3 Plasma lipoprotein profile of control and *Cyp8b1*$^{-/-}$ mice

Fasting plasma lipoproteins including total cholesterol (TC), HDL cholesterol (HDLc) and triglycerides (TG) were quantified from both control and *Cyp8b1*$^{-/-}$ mice. n= 7-11. Data expressed as mean±SEM. *p< 0.05 by Student's t-test.

To determine whether the increase in HDL cholesterol in *Cyp8b1*$^{-/-}$ mice is attributed to the change in the levels of hepatic ATP- binding cassette transporter (ABCA1) and scavenger receptor class B member 1 (SR-B1), we quantified hepatic mRNA expression of both these genes in HCD fed control and *Cyp8b1*$^{-/-}$ mice. ABCA1 mediates the cellular efflux of

phospholipids and cholesterol to lipid-poor apolipoprotein A1 (apoA1) and plays a significant role in HDL metabolism while SR-B1 functions as HDL receptor in the liver. We observed a trend towards an increase in the expression of ABCA1 while there was no change in SR-B1 expression in the *Cyp8b1*$^{-/-}$ mice. Unchanged expression of SREBP-1c may explain the lack of change in plasma TG levels of the *Cyp8b1*$^{-/-}$ mice compared to their control littermates (Figure 3.1A).

Quantification of hepatic mRNA of genes involved in bile acid synthesis revealed that the gene expression of *Cyp7a1* was significantly higher in *Cyp8b1*$^{-/-}$ mice compared to the controls, while there was no change in the gene expression of *Cyp27a1*. In addition, the *Cyp8b1*$^{-/-}$ mice show complete knockdown of *Cyp8b1* gene expression compared to control mice (Figure 3.1B). These findings are also in line with previously published data (38).

Figure 3.1

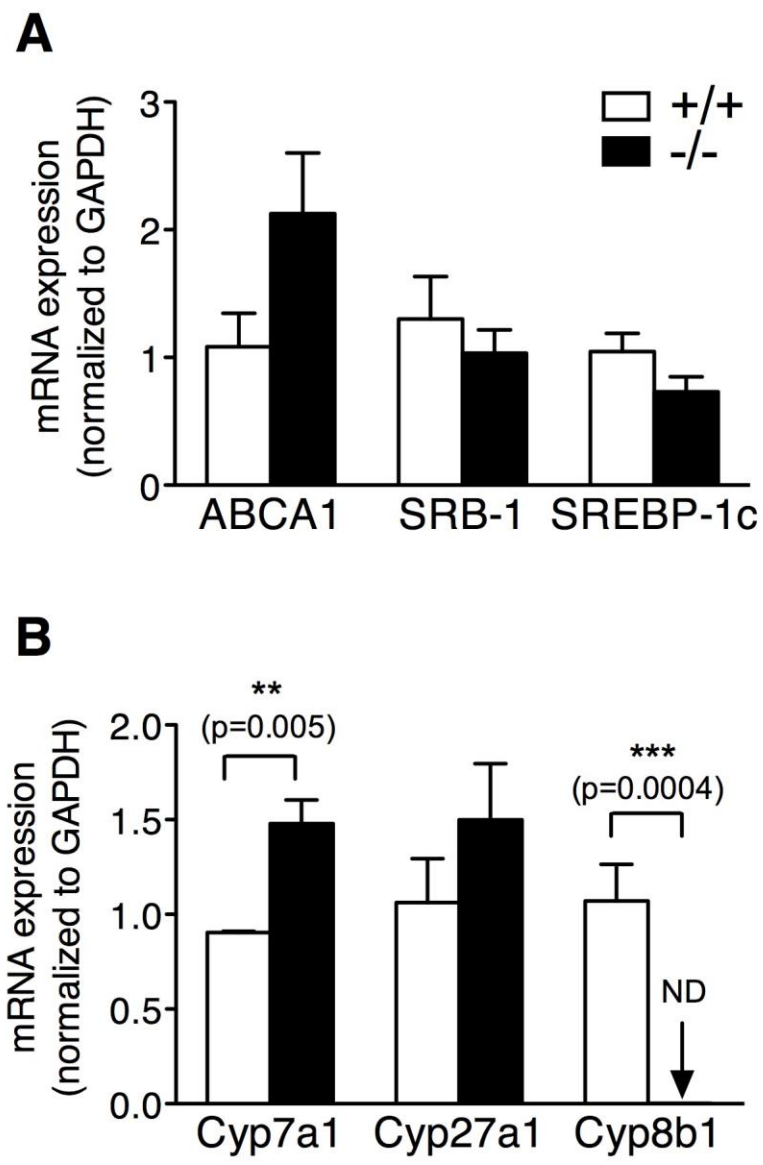

Figure 3.1 No changes in mRNA expression of genes involved in lipid metabolism, whereas significant changes are observed in bile acid synthesis genes of *Cyp8b1*$^{-/-}$ mice

- **A.** Hepatic expression of *Abca1*, *Sr-b1* and *Srebp1c* in control (+/+) and *Cyp8b1*$^{-/-}$ (-/-) mice challenged with 0.5% cholesterol diet (HCD) for 4 weeks. Data shown as mean ± SEM; n= 4-5.
- **B.** Hepatic expression of *Cyp7a1*, *Cyp27a1* and *Cyp8b1* in control (+/+) and *Cyp8b1*$^{-/-}$ (-/-) mice challenged with 0.5% cholesterol diet (HCD) for 4 weeks. Data shown as mean ± SEM; n= 4-5; ND- not detectable, **p<0.01 and ***p<0.001 by Student's t-test.

3.2 *Cyp8b1*$^{-/-}$ mice have reduced fat absorption

The main function of bile acids is to facilitate micelle formation, and promote dietary fat absorption. We observed reduced body weight in *Cyp8b1*$^{-/-}$ mice fed HCD (p=0.006) (Figure 3.2A) primarily due to decreased adipose depot weights (Figure 3.2B). This suggests that altered bile acid composition in these mice may contribute to reduced dietary fat absorption.

To further determine the consequence of the *Cyp8b1* deletion on fat absorption, we performed oral fat tolerance tests by quantifying plasma triglyceride levels after an intragastric gavage of corn oil in both *Cyp8b1*$^{-/-}$ mice and their control littermates. As expected, the *Cyp8b1*$^{-/-}$ mice showed significant reduction in fat absorption compared to their control littermates (~18% reduced area under the curve (AUC)) (Figure 3.2C). These data show that the altered bile acid profile of the *Cyp8b1*$^{-/-}$ mice (38) leads to defective intestinal fat absorption in addition to the reported reduction in cholesterol absorption (38,40).

3.3 *Cyp8b1*$^{-/-}$ mice display improved glycemic control

By acting as signaling molecules for both FXR and TGR5, bile acids are involved in maintaining glucose metabolism and insulin sensitivity (50). Previous studies have shown that *Cyp8b1*$^{-/-}$ mice have an altered bile acid pool size (38), and this change in the bile acid pool may be expected to result in altered glucose homeostasis. We measured fasting glucose and insulin levels in *Cyp8b1*$^{-/-}$ mice and did not observe changes in mice fed regular chow diet (Figures 3.3A and 3.4A). However, *Cyp8b1*$^{-/-}$ mice fed HCD showed a marked reduction in fasting plasma glucose levels compared to controls (p=0.003) (Figure 3.3A). We next performed oral glucose

tolerance tests (OGTT) and found that *Cyp8b1*$^{-/-}$ mice were significantly more glucose tolerant compared to controls fed HCD (AUC p=0.04) (Figure 3.3B).

Increased insulin secretion after an oral glucose load is due in part to the action of incretins, an effect that is diminished in type 2 diabetes (51). To investigate the possible alterations in incretin actions of *Cyp8b1*$^{-/-}$ mice, we performed both intra-peritoneal glucose tolerance test (IPGTT) and an OGTT. Interestingly, the *Cyp8b1*$^{-/-}$ mice showed significantly improved insulin response to oral compared to IP glucose load (ANOVA p=0.01, AUC p=0.002) (Figure 3.3C), suggesting that incretin hormones may be responsible for the improved glycemic response.

Recent evidence suggests an association between increased 12α-hydroxy bile acids and insulin resistance in humans (52). In addition, mice overexpressing *Cyp7a1* are protected against diet-induced obesity and insulin resistance (23). Since *Cyp8b1*$^{-/-}$ mice lack 12α-hydroxy bile acids and express increased hepatic *Cyp7a1* transcripts (Figure 1B) (38), we assessed insulin sensitivity in these mice. On HCD, *Cyp8b1*$^{-/-}$ mice showed an almost ~76% reduction in fasting insulin levels compared to controls (p=0.020) (Figure 3.4A). Blood glucose levels of *Cyp8b1*$^{-/-}$ and control mice were also quantified following the IP injection of insulin. Knockout mice fed HCD were highly insulin sensitive compared to controls on the same diet (ANOVA p=0.003, AUC p=0.0007) (Figure 3.4B). In addition, quantification of HOMA-IR index showed that the *Cyp8b1*$^{-/-}$ mice were significantly more insulin sensitive compared to the control mice (p=0.011) (Figure 3.4C).

Figure 3.2

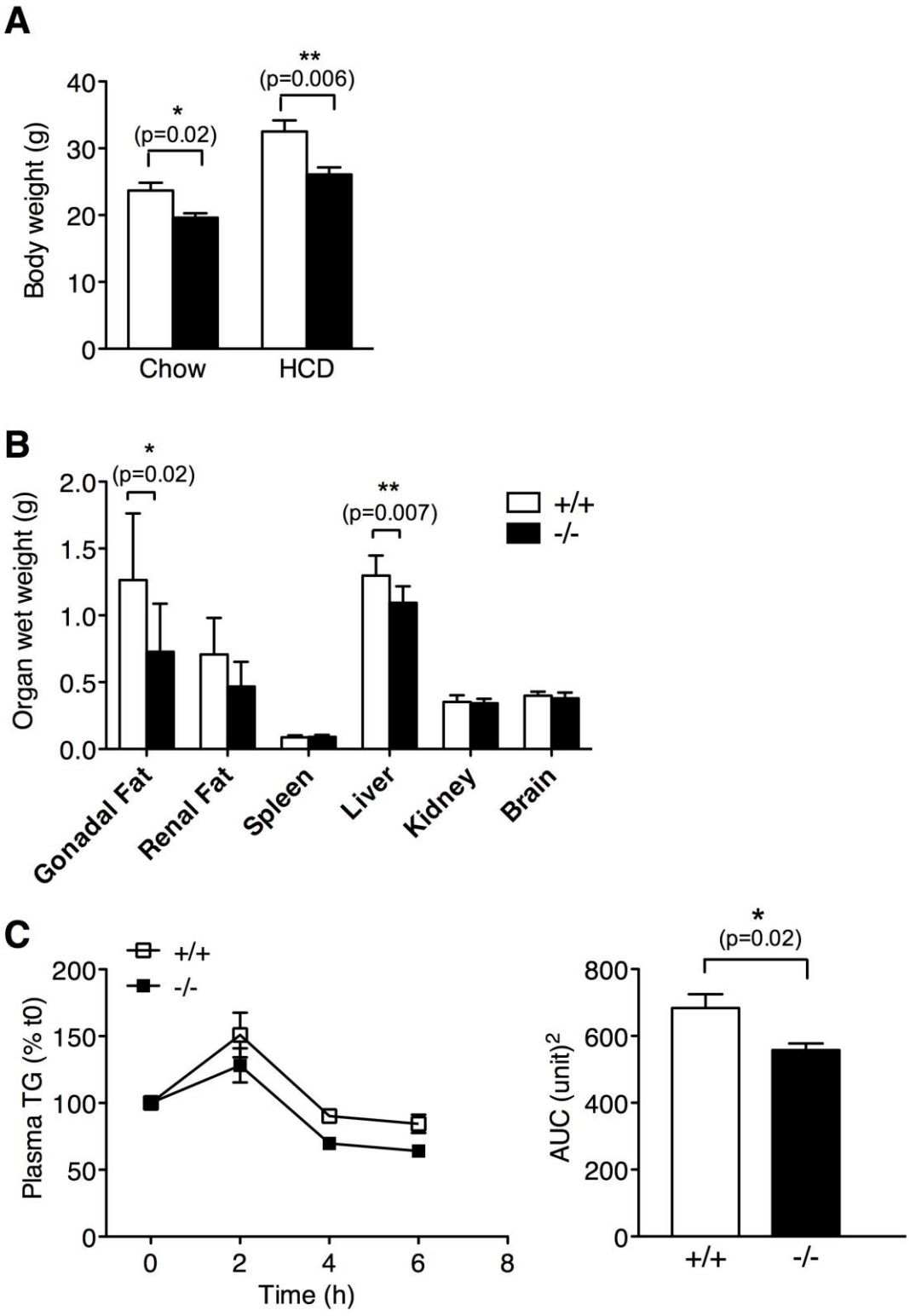
A
Body weight (g)
40
30
20
10
0
*
(p=0.02)
**
(p=0.006)
Chow
HCD
B
Organ wet weight (g)
2.0
1.5
1.0
0.5
0.0
*
(p=0.02)
**
(p=0.007)
+/+
-/-
Gonadal Fat
Renal Fat
Spleen
Liver
Kidney
Brain
C
Plasma TG (% t0)
200
150
100
50
0
+/+
-/-
0
2
4
6
8
Time (h)
AUC (unit)2
800
600
400
200
0
*
(p=0.02)
+/+
-/-

Figure 3.2 *Cyp8b1*$^{-/-}$ mice have reduced fat absorption

A. Body weight was measured for control (+/+) and *Cyp8b1*$^{-/-}$ (-/-) mice fed regular chow and 0.5% cholesterol diet (HCD) for 4 weeks. Data expressed as mean± SEM; n=7; **p<0.01 by Student's t-test.

B. Organ wet weights were measured in control (+/+) and *Cyp8b1*$^{-/-}$ (-/-) mice fed HCD for 4 weeks. Data expressed as mean± SEM; n=9; *p<0.05 and **p<0.01 by Student's t-test.

C. Chow fed 3-month-old control (+/+) and *Cyp8b1*$^{-/-}$ (-/-) mice were subjected to an oral fat tolerance test. Data for area under the curve (AUC) shown as mean ± SEM, n=7, *p<0.05 by Student's t-test.

Figure 3.3

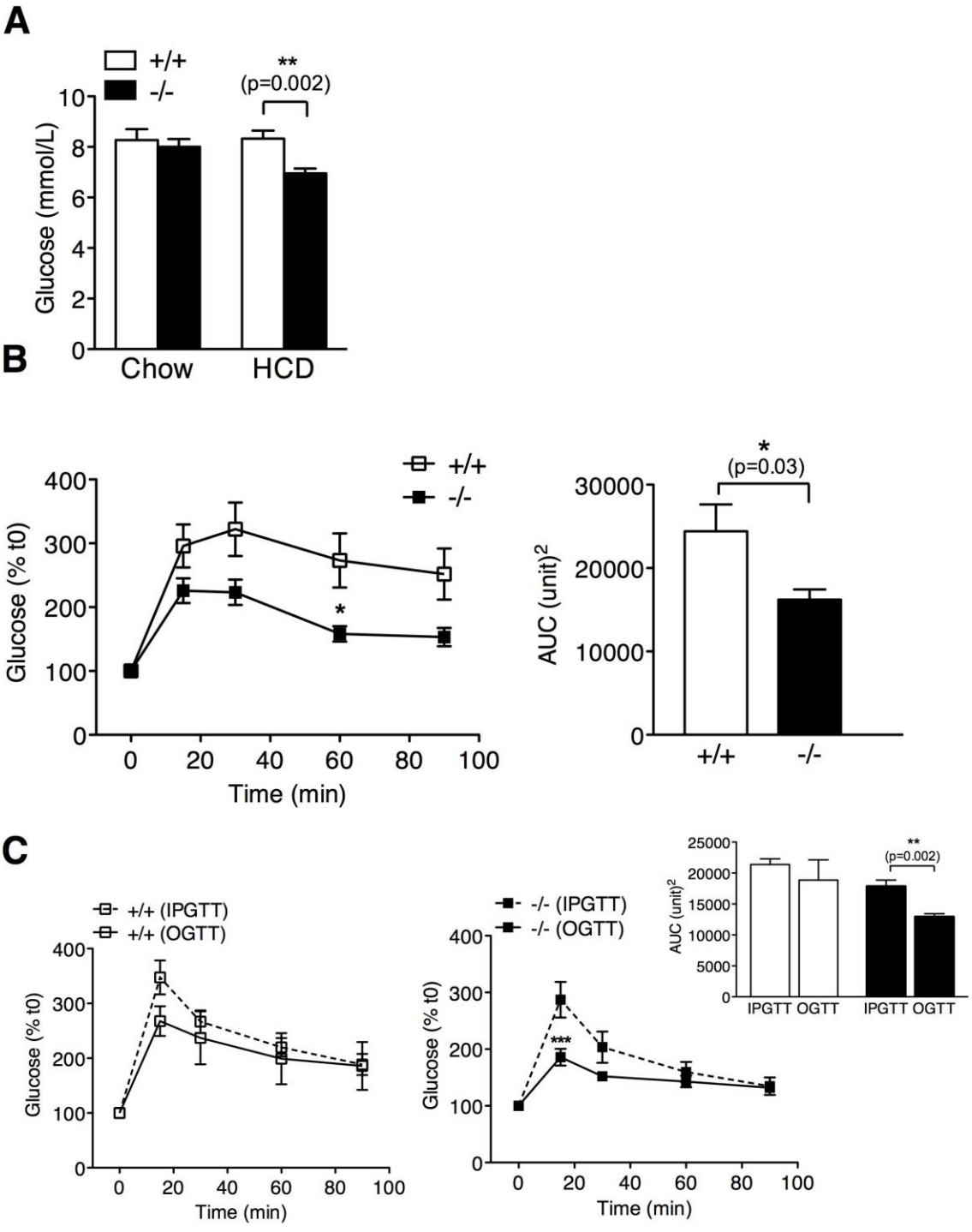
A
+/+
-/-
**
(p=0.002)
Glucose (mmol/L)
Chow
HCD
B
+/+
-/-
Glucose (% t0)
Time (min)
*
(p=0.03)
AUC (unit)²
C
+/+ (IPGTT)
+/+ (OGTT)
-/- (IPGTT)
-/- (OGTT)
***
IPGTT OGTT IPGTT OGTT

Figure 3.3 *Cyp8b1*$^{-/-}$ mice have improved glycemic profile

A. Baseline glucose was measured after 4h fasting for control (+/+) and *Cyp8b1*$^{-/-}$ (-/-) mice fed regular chow and 0.5% cholesterol diet (HCD) for 4 weeks. Data expressed as mean± SEM; n=7-11; **p<0.01 by Student's t-test.

B. Oral glucose tolerance test (OGTT) along with AUC from control (+/+) and *Cyp8b1*$^{-/-}$ (-/-) mice fed HCD for 4 weeks. Data are shown as mean ± SEM; n=6; *p<0.05 by two-way ANOVA followed by the Bonferroni post-hoc test, AUC *p=0.04 by Student's t-test.

C. Comparison between control (+/+) and *Cyp8b1*$^{-/-}$ (-/-) mice fed HCD for their respective intraperitoneal glucose tolerance test (IPGTT) and oral glucose tolerance test (OGTT) with corresponding area under the curve (AUC). Data expressed as mean± SEM; n=5-7; ***p<0.001 by two-way ANOVA followed by the Bonferroni post-hoc test and for AUC **p<0.01 by Student's t-test.

It is known that insulin resistance results in dysregulated hepatic gluconeogenesis. Furthermore, the study of *Cyp7a1* overexpressing mice also showed that the improved insulin sensitivity in these transgenic mice may be attribute to reduced fasting hepatic gluconeogenesis (44). Hence, we also quantified the mRNA transcript levels of genes involved in gluconeogenesis - *G6pase* and *Pepck*, in both control and *Cyp8b1*$^{-/-}$ livers. There was no difference in the gene expression of *G6Pase* and *Pepck* of the *Cyp8b1*$^{-/-}$ mice (Figure 3.4D), suggesting that the improved glucose homeostasis in the *Cyp8b1*$^{-/-}$ mice could not be attributed to reduced gluconeogenesis.

3.4 *Cyp8b1*$^{-/-}$ mice have increased GLP-1 release

Incretin hormones are secreted in response to nutrient ingestion and FFAs activate their release (53). Our observation of reduced fat absorption led us to hypothesize that increased FFAs may persist in the intestinal lumen of *Cyp8b1*$^{-/-}$ mice. This led us to investigate if *Cyp8b1*$^{-/-}$ mice have increased luminal free fatty acid content. We harvested different intestinal sections (duodenum, jejunum and ileum) of mice gavaged with liquefied high fat diet, and measured the free fatty acid content in each of these sections. We observed that the *Cyp8b1*$^{-/-}$ mice have significantly increased free fatty acids in their ileal lumen compared to their control littermates ($p=0.03$) (Figure 3.5A).

Since FFA are known to potentiate the release both of the incretins, GIP and GLP-1, we measured plasma levels of these hormones 30 min post-oral glucose load in the *Cyp8b1*$^{-/-}$ and control mice. We did not observe significant differences in the total plasma GIP levels between the two groups fed HCD (Figure 3.5B). We next assessed plasma GLP-1 in these mice. On HCD,

Cyp8b1$^{-/-}$ mice showed ~80% increase in their plasma total GLP-1 levels, compared to controls ($p=0.04$) (Figure 3.5C). We also found higher *Glp-1* gene expression in the ilea of these mice ($p=0.03$) (Figure 3.5D). These results were consistent with our observation of increased FFA content in the ileal lumen of the *Cyp8b1*$^{-/-}$ mice.

Since the role of TGR5 in activating GLP-1 release is well characterized (24,25), we also assessed transcript levels of *Tgr5* in the ileum and the colon (Figure 3.5E) of these mice. There was a trend to increased *Tgr5* transcript levels in the colon, but it was not significant ($p>0.05$, $n=10$) in *Cyp8b1*$^{-/-}$ mice. Also the ileal transcripts did not show any change. Thereby suggesting that it is the change in free fatty acid content of the ileal lumen that is responsible for increase in GLP-1 secretion in *Cyp8b1*$^{-/-}$ mice.

Figure 3.4

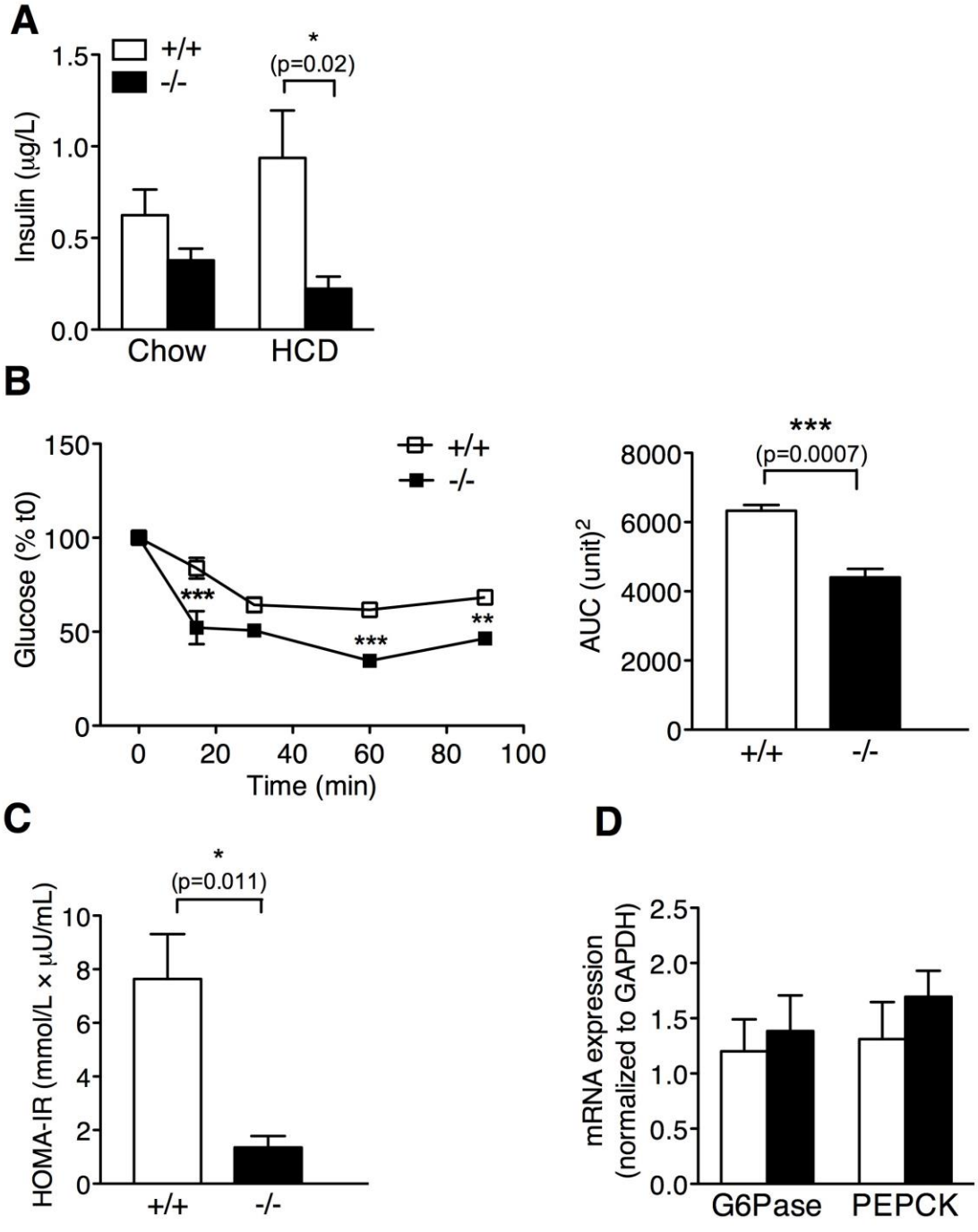
A
+/+
-/-
*
(p=0.02)
Insulin (μg/L)
1.5
1.0
0.5
0.0
Chow
HCD
B
+/+
-/-
Glucose (% t0)
150
100
50
0
***
***
**
0
20
40
60
80
100
Time (min)
***
(p=0.0007)
AUC (unit)²
8000
6000
4000
2000
0
+/+
-/-
C
*
(p=0.011)
HOMA-IR (mmol/L x μU/mL)
10
8
6
4
2
0
+/+
-/-
D
mRNA expression
(normalized to GAPDH)
2.5
2.0
1.5
1.0
0.5
0.0
G6Pase
PEPCK

Figure 3.4 *Cyp8b1*$^{-/-}$ mice have enhanced insulin sensitivity

A. Baseline insulin was measured after 4h fasting for control (+/+) and *Cyp8b1*$^{-/-}$ (-/-) mice fed regular chow and 0.5% cholesterol diet (HCD) for 4 weeks. Data expressed as mean± SEM; n=7-11; *p<0.05 by Student's t-test.

B. Intraperitoneal insulin tolerance test (IPITT) along with AUC from control (+/+) and *Cyp8b1*$^{-/-}$ (-/-) mice fed HCD for 4 weeks. Data shown as mean ± SEM; n=4-5; *p=0.02 by Student's t-test; for IPITT *p<0.05, **p<0.01, ***p<0.001 by two-way ANOVA followed by the Bonferroni post-hoc test, and AUC ***p<0.001 by Student's t-test.

C. Homeostatis model assessment of insulin resistance (HOMA-IR) was assessed for control (+/+) and *Cyp8b1*$^{-/-}$ (-/-) mice fed HCD for 4 weeks. Data expressed as mean± SEM; n=4; *p<0.05 by Student's t-test.

D. Hepatic expression of *G6Pase* and *Pepck* in control (+/+) and *Cyp8b1*$^{-/-}$ (-/-) mice challenged with HCD for 4 weeks. Data shown as mean ± SEM; n= 4-5.

Figure 3.5

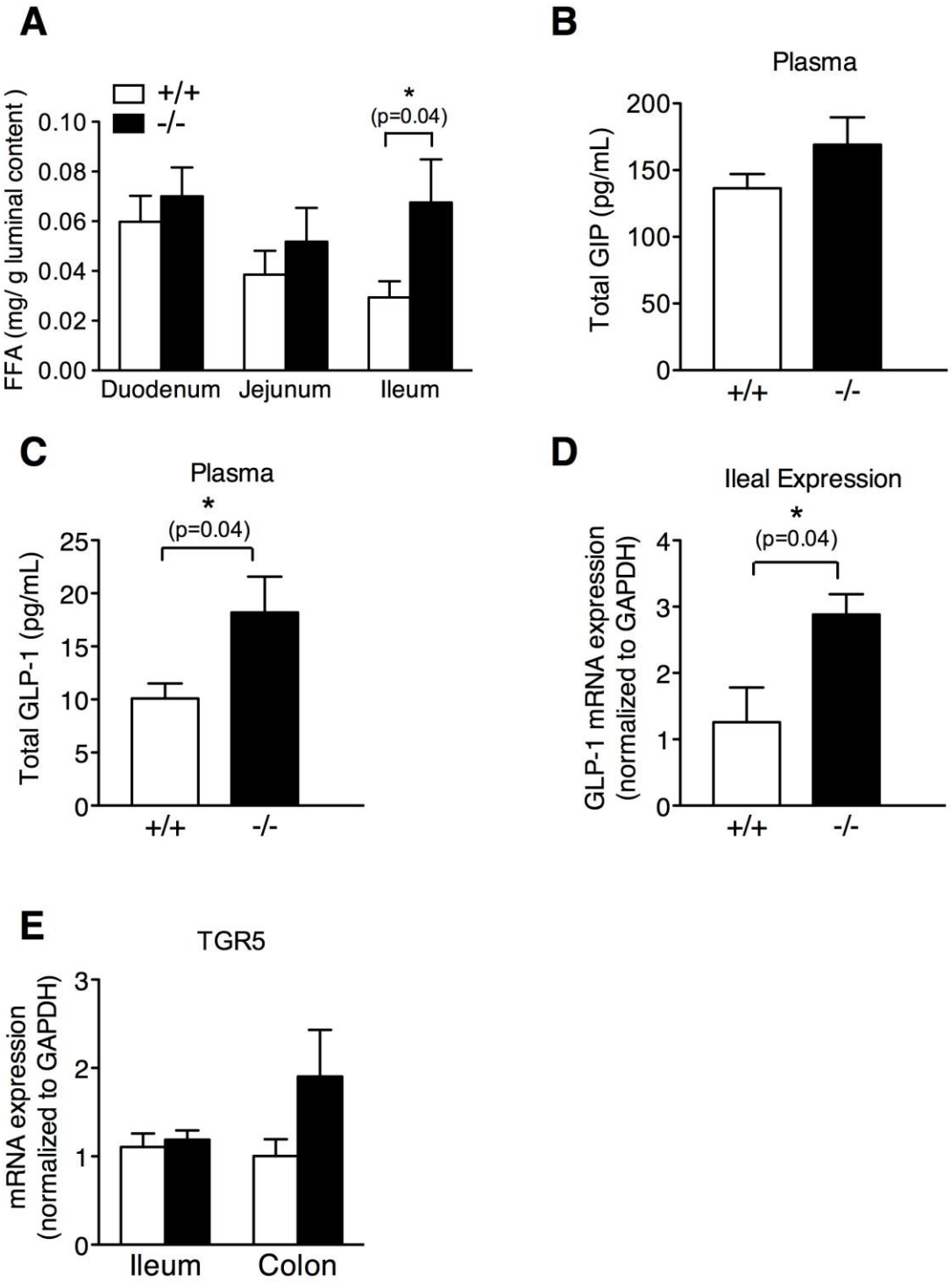
A
+/+
-/-
*
(p=0.04)
FFA (mg/ g luminal content)
0.10
0.08
0.06
0.04
0.02
0.00
Duodenum
Jejunum
Ileum
B
Plasma
Total GIP (pg/mL)
200
150
100
50
0
+/+
-/-
C
Plasma
*
(p=0.04)
Total GLP-1 (pg/mL)
25
20
15
10
5
0
+/+
-/-
D
Ileal Expression
*
(p=0.04)
GLP-1 mRNA expression
(normalized to GAPDH)
4
3
2
1
0
+/+
-/-
E
TGR5
mRNA expression
(normalized to GAPDH)
3
2
1
0
Ileum
Colon

Figure 3.5 *Cyp8b1*$^{-/-}$ mice have increased GLP-1 levels

A. Luminal free fatty acid (FFA) content from the intestinal regions of control (+/+) and *Cyp8b1*$^{-/-}$ (-/-) mice post oral gavage of liquefied high fat diet (HFD). Data shown as mean ± SEM; n=9; *p<0.05 by Student's t-test.

B. Plasma levels of GIP in control (+/+) and *Cyp8b1*$^{-/-}$ (-/-) mice 30 min post-oral glucose gavage. Data shown as mean ± SEM; n= 9-10.

C. Plasma levels of GLP-1 in control (+/+) and *Cyp8b1*$^{-/-}$ (-/-) mice 30 min post-oral glucose gavage, challenged with 0.5% cholesterol diet (HCD) for 4 weeks. Data shown as mean ± SEM; n= 9-10; *p<0.05 by Student's t-test.

D. Ileal expression of Glp-1 in control (+/+) and *Cyp8b1*$^{-/-}$ (-/-) mice challenged with HCD for 4 weeks. Data shown as mean ± SEM; n=5; *p<0.05 by Student's t-test.

E. Gene expression of *Tgr5* transcripts in the ileum and colon of control (+/+) and *Cyp8b1*$^{-/-}$ (-/-) mice challenged with HCD for 4 weeks. Data shown as mean ± SEM; n=9-11.

3.5 *Cyp8b1*$^{-/-}$ mice have improved β-cell function

One well established physiological effect of GLP-1 is to stimulate insulin secretion from β-cells in the islets. Since we found higher GLP-1 release in *Cyp8b1*$^{-/-}$ mice, we measured insulin secretion in response to oral glucose load, and found it to be significantly higher in *Cyp8b1*$^{-/-}$ mice compared to control mice on the HCD (Figure 3.6A). GLP-1 is also known to stimulate the transcription of the proinsulin gene, thereby increasing insulin biosynthesis (54). Insulin content in *Cyp8b1*$^{-/-}$ islets was found to be markedly higher than in control islets (p=0.03) (Figure 3.6B). To determine if the increased islet insulin content contributed to *in vivo* insulin secretion in these mice, we performed *ex vivo* glucose stimulated insulin secretion (GSIS) on freshly isolated islets. A trend to increased insulin secretion from the *Cyp8b1*$^{-/-}$ islets in response to high glucose was observed (p=0.06) (Figure 3.6C).

Mice lacking *Cyp8b1* did not demonstrate any change in β-cell mass (Figure 3.6D-E). It is essential to note that pharmacological but not physiological doses of GLP-1 have previously been reported to increase β-cell mass in rats and diabetic mice (55-57). These findings show that β-cell function is enhanced in mice lacking *Cyp8b1*, associated with an increase in circulating levels of GLP-1.

3.6 GLP-1 receptor antagonism normalizes glucose tolerance in *Cyp8b1*$^{-/-}$ mice

We next investigated if GLP-1 was an important contributor to the observed improvement in β-cell function of *Cyp8b1*$^{-/-}$ mice. Exendin (9-39) amide (Ex-3) is a GLP-1 receptor antagonist that impacts β-cell function and glucose metabolism in healthy subjects (58). We performed an OGTT in *Cyp8b1*$^{-/-}$ and control mice fed HCD, administered with Ex-3 or vehicle. As expected,

Ex-3 treated controls showed impaired glucose tolerance compared to vehicle treated controls on HCD (Figure 3.7A). Interestingly, GLP-1 receptor antagonism in HCD fed *Cyp8b1*$^{-/-}$ mice normalized the observed improvement in glucose tolerance similar to levels seen in vehicle treated control mice (Figure 3.7B). This is due to the competitive inhibition that Ex-3 exerts on GLP-1 for binding with the GLP-1r, suggesting that GLP-1 indeed plays a crucial role in improving the glucose tolerance of *Cyp8b1*$^{-/-}$ mice.

Figure 3.6

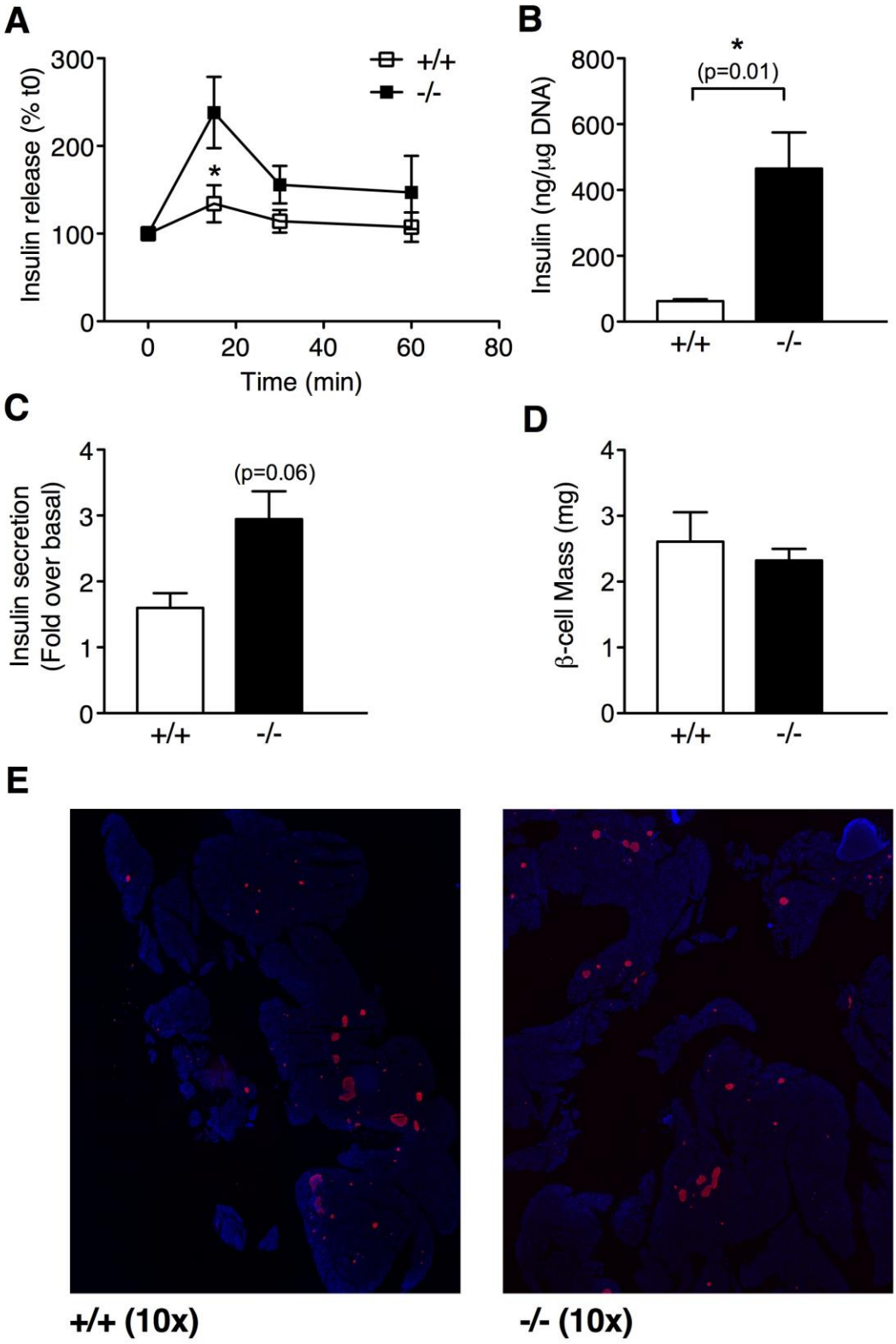
A
Insulin release (% t0)
300
200
100
0
+/+
-/-
*
0
20
40
60
80
Time (min)
B
Insulin (ng/μg DNA)
800
600
400
200
0
*
(p=0.01)
+/+
-/-
C
Insulin secretion
(Fold over basal)
4
3
2
1
0
(p=0.06)
+/+
-/-
D
β-cell Mass (mg)
4
3
2
1
0
+/+
-/-
E
+/+ (10x)
-/- (10x)

Figure 3.6 *Cyp8b1*$^{-/-}$ mice have improved islet insulin secretion

- **A.** *In vivo* glucose stimulated insulin secretion for 4 week 0.5% cholesterol diet (HCD) fed control (+/+) and *Cyp8b1*$^{-/-}$ (-/-) mice post-oral glucose load, after 4h fasting. Data shown as mean ± SEM; n= 7; *p<0.05 by two-way ANOVA followed by the Bonferroni post-hoc test.
- **B.** Islet insulin content in control (+/+) and *Cyp8b1*$^{-/-}$ (-/-) mice. Data shown as mean ± SEM; n=4; *p=0.014 by Student's t-test.
- **C.** Fold over basal insulin secretion from isolated islets post-exposure to 16mM glucose. Data expressed as mean± SEM; n=4.
- **D.** β-cell mass was measured by calculating the percentage of insulin-positive surface area from evenly spaced slides per pancreas then multiplying with the pancreatic weight for control (+/+) and *Cyp8b1*$^{-/-}$ (-/-) mice. Data expressed as mean± SEM; n=4.
- **E.** Representative pancreas sections of control (+/+) and *Cyp8b1*$^{-/-}$ (-/-) mice positively stained for insulin and counterstained with DAPI. Images at 10x magnification (objective).

Figure 3.7

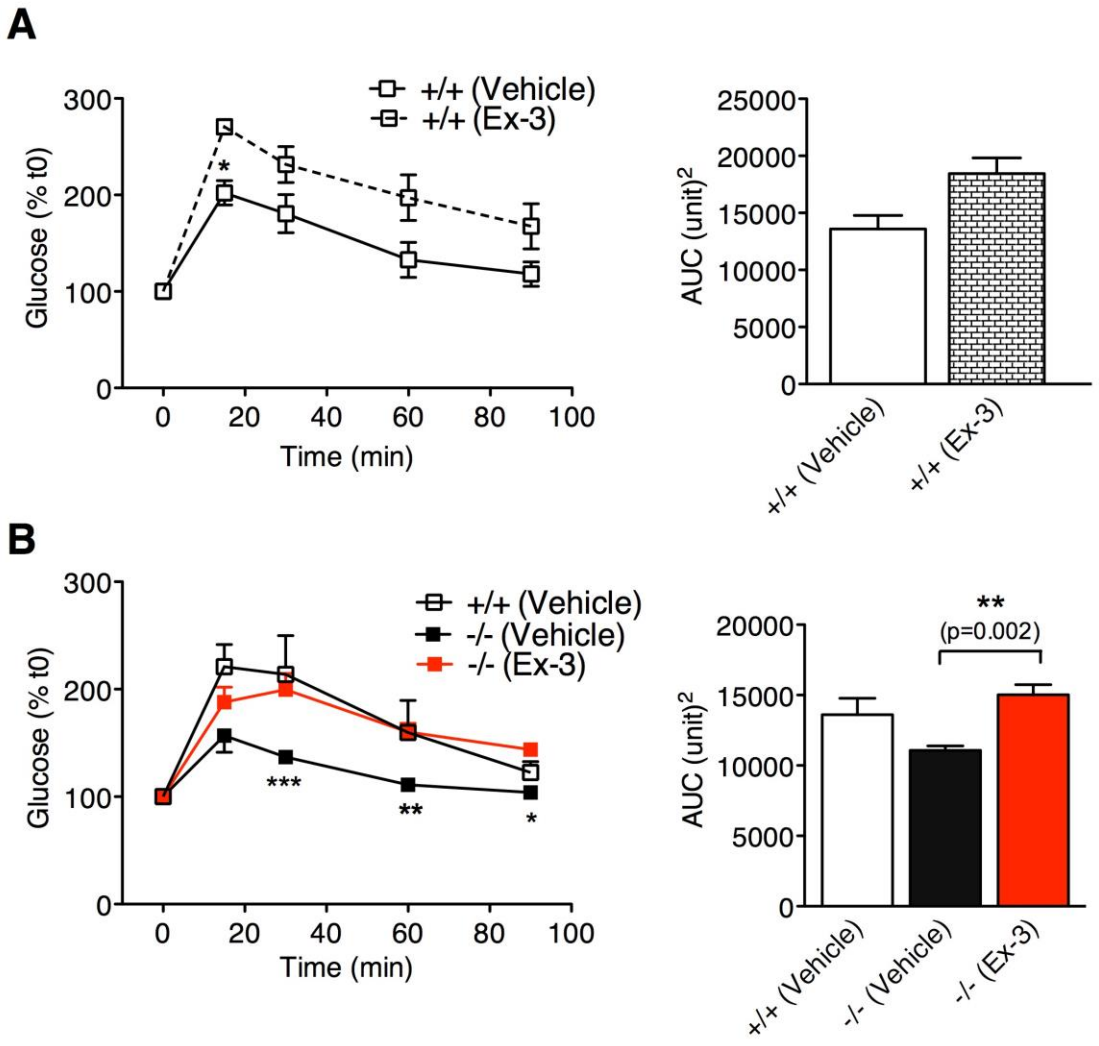

Figure 3.7 Normalized glucose tolerance following GLP-1 receptor antagonism in *Cyp8b1*$^{-/-}$ mice

A. Four week 0.5% cholesterol diet (HCD) fed control (+/+) mice were treated either with 167 μg/kg body weight of Exendin-3 (Ex-3) or vehicle (PBS) and OGTT was performed. Data shown as mean ± SEM; n=4; *p<0.05 by two-way ANOVA followed by the Bonferroni post-hoc test.

B. Four week HCD fed control (+/+) and *Cyp8b1*$^{-/-}$ (-/-) mice were treated either with 167 μg/kg body weight of Exendin-3 (Ex-3) or vehicle (PBS) and OGTT was performed. Data shown as mean ± SEM; n=4; *p<0.05, **p<0.01, ***p<0.001 by two-way ANOVA followed by the Bonferroni post-hoc test, and AUC for OGTT **p<0.01 by Student's t-test.

3.7 *Cyp8b1*$^{-/-}$ mice display altered levels of circulating bile acids

Recent evidence that bile acid induced activation of TGR5 on β-cells promotes insulin release (59) lead us to hypothesize that the change in the bile acid pool of *Cyp8b1*$^{-/-}$ mice could also improve islet function directly. Previous studies have shown that *Cyp8b1*$^{-/-}$ mice display an overall increased bile acid pool, with complete absence of CA and relative enrichment of other bile acids (38). However, changes in the circulatory bile acid profile of *Cyp8b1*$^{-/-}$ mice have not been reported. Therefore we quantified plasma bile acids in the *Cyp8b1*$^{-/-}$ mice. No CA was detected and CDCA levels were unchanged in the plasma of *Cyp8b1*$^{-/-}$ mice. We hypothesized that in the absence of *Cyp8b1,* the bile acid pathway would be shifted from CA to CDCA synthesis, resulting in increased plasma CDCA. However, the unchanged CDCA levels may be explained by efficient conversion of excess CDCA to MCA, since our mice lacking *Cyp8b1* have increased plasma levels of αMCA (8-fold increase; p=0.002), β-MCA (4-fold increase; p=0.002) and ω-MCA (2-fold increase; p=0.02), compared to control mice (Figure 3.8A). In addition, *Cyp8b1*$^{-/-}$ mice have a significant, almost 4 fold increase in circulating levels of ursodeoxycholic acid (UDCA) (p=0.002), compared to the controls (Figure 3.8A). Overall changes in the plasma bile acid profile were similar to those reported previously in bile of *Cyp8b1*$^{-/-}$ mice (38).

3.8 Administration of bile acids does not alter glucose tolerance in wild-type mice

To assess whether the alterations in peripheral bile acid species may also directly contribute to the observed improvement in β-cell function, we administered a cocktail containing αMCA, βMCA, ωMCA and UDCA, the significantly increased circulating bile acids of *Cyp8b1*$^{-/-}$ mice, to wild-type mice, followed by IPGTT. No difference in glucose tolerance between the bile acid

and vehicle treated mice was observed (Figure 3.8B). Thus, the increased peripheral bile acids may not play a major role in the improved glucose tolerance observed in the *Cyp8b1*$^{-/-}$ mice.

Figure 3.8

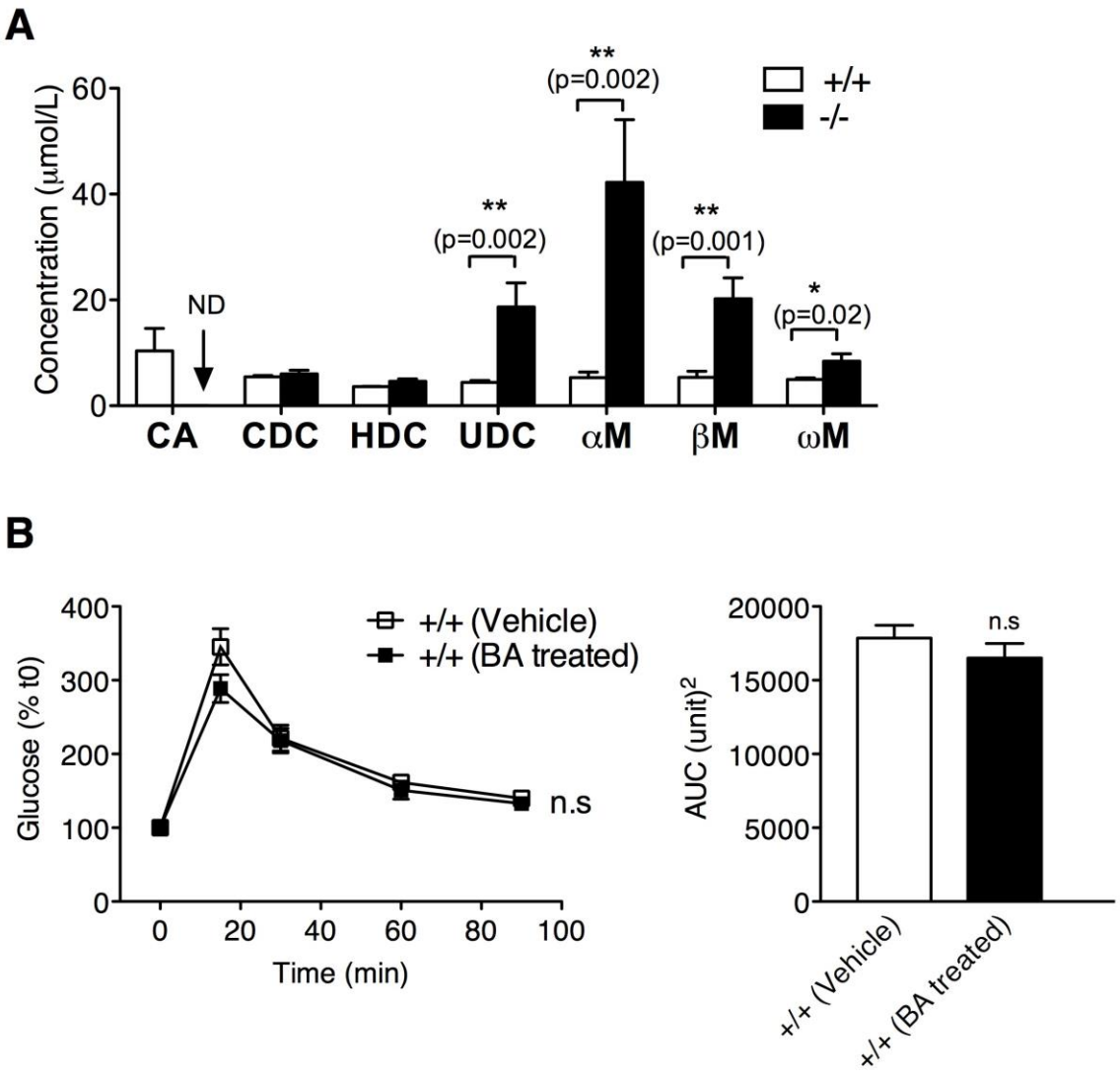

Figure 3.8 *Cyp8b1*$^{-/-}$ mice have altered circulating bile acid pool and wild-type mice exhibit no change in glucose tolerance post bile acid treatment

- **A.** Plasma bile acid pool in control (+/+) and *Cyp8b1*$^{-/-}$ (-/-) mice fed 0.5% cholesterol diet (HCD) for 4 weeks where CA-cholic acid, CDC- chenodeoxycholic acid, HDC-hyodeoxycholic acid, UDC-ursodeoxycholic acid, α/β/ω MCA- α/β/ω muricholic acid. ND- not detectable, Data shown as mean± SEM; n=4; *p< 0.05, **p<0.01 by Student's t-test.
- **B.** IPGTT was performed in vehicle or bile acid treated (0.125 mg/kg of αMCA, 0.028 mg/kg of βMCA, 4.96 μg/kg of ωMCA and 0.011 mg/kg of UDCA) wild-type mice. Data shown as mean± SEM; n=5, n.s- not significant.

3.9 CA treatment abolishes the improvement in glucose tolerance of *Cyp8b1*$^{-/-}$ mice

The consequences of the loss of *Cyp8b1* are not only an increase in MCA and UDCA but also a complete loss of cholate and its secondary metabolites in the bile. To dissect the contribution of CA in the manifestation of the improved phenotype, we treated *Cyp8b1*$^{-/-}$ mice with CA or vehicle. Interestingly, the observed reduction in fat absorption of *Cyp8b1*$^{-/-}$ mice was normalized upon CA administration (Figure 3.9A). Next, we gavaged CA to *Cyp8b1*$^{-/-}$ mice for 3 consecutive days, followed by a measurement of glucose tolerance. CA treatment of *Cyp8b1*$^{-/-}$ mice reversed the glucose tolerance, which reached levels similar to that of vehicle treated controls (Figure 3.9B). Interestingly, plasma GLP-1 levels 30 min post oral glucose gavage of the CA treated *Cyp8b1*$^{-/-}$ mice were also normalized to that of the vehicle treated control (Figure 3.9C). Together, these data suggest that the absence of CA contributes to the improved glucose tolerance in mice lacking *Cyp8b1*.

Figure 3.9

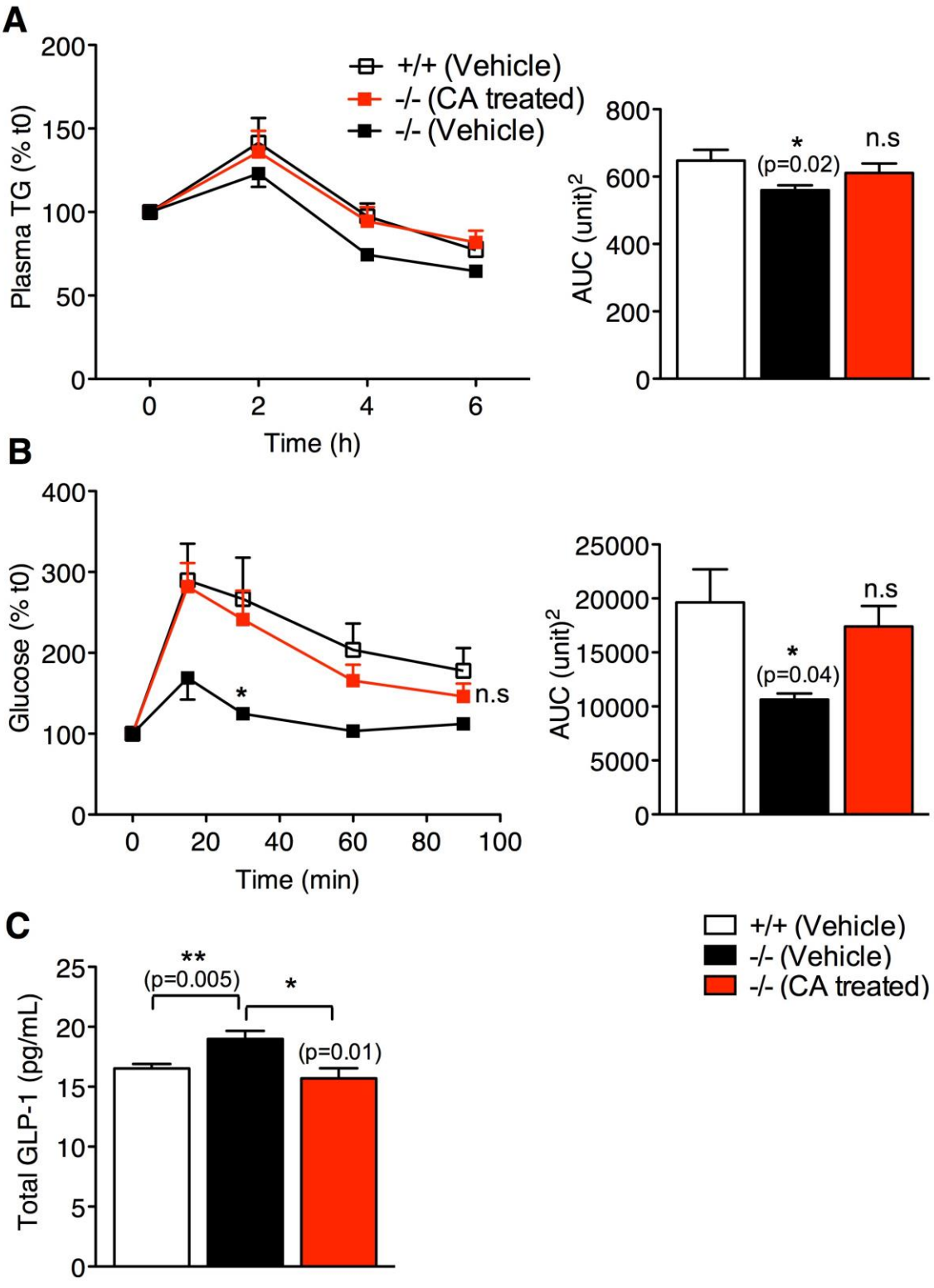
A
+/+ (Vehicle)
-/- (CA treated)
-/- (Vehicle)
Plasma TG (% t0)
Time (h)
AUC (unit)2
*
(p=0.02)
n.s
B
Glucose (% t0)
Time (min)
*
n.s
AUC (unit)2
*
(p=0.04)
n.s
C
Total GLP-1 (pg/mL)
**
(p=0.005)
*
(p=0.01)
+/+ (Vehicle)
-/- (Vehicle)
-/- (CA treated)

Figure 3.9 Treatment with CA normalizes plasma glucose response in *Cyp8b1*$^{-/-}$ mice

A. Oral fat tolerance in control (+/+) and *Cyp8b1*$^{-/-}$ (-/-) mice post oral gavage of 17 mg/kg CA or vehicle. Data shown as mean ± SEM; n=6; significance for AUC measured with respect to vehicle treated controls, *p<0.05 by Student's t-test, n.s- not significant.

B. IPGTT in control (+/+) and *Cyp8b1*$^{-/-}$ (-/-) mice fed 0.5% cholesterol diet (HCD), post 3-day oral gavage of 17 mg/kg CA or vehicle treatment. Data shown as mean± SEM; n=6; significance for AUC measured with respect to vehicle treated controls, *p<0.05 by Student's t-test, n.s- not significant.

C. Plasma levels of GLP-1 in control (+/+) and *Cyp8b1*$^{-/-}$ (-/-) mice fed HCD, post 3-day oral gavage of 17 mg/kg CA or vehicle. Data shown as mean ± SEM; n=5-9; *p<0.05, **p<0.01 and by Student's t-test.

Chapter 4: Discussion

Mice with targeted disruption of the P450 cytochrome *Cyp8b1* have reduced intestinal cholesterol absorption and accumulation of cholesterol esters in their livers. These mice also have increased synthesis of bile acids as a result of the up-regulation of the hepatic Cyp7a1 pathway (38). Previous studies have focused on cholesterol metabolism in *Cyp8b1*$^{-/-}$ mice. However the impact of the absence of *Cyp8b1* on glucose homeostasis is not well studied. Our study is the first to demonstrate that absence of *Cyp8b1* in mice and the consequent changes in bile acid metabolism result in significant improvement in both glucose tolerance and β-cell function. This effect appears to be primarily mediated by an increase in GLP-1 secretion and subsequent improvement in islet insulin secretion.

Our findings also show that genetic ablation of 12α-hydroxylated bile acid synthesis results in improved insulin sensitivity. This is in agreement with a recent finding of association of 12α-hydroxylated bile acids with insulin resistance in humans (52). Thus, our data adds to the current knowledge of the phenotype of *Cyp8b1*$^{-/-}$ mice and elucidates the impact of bile acids on glucose metabolism.

By measuring the plasma lipoproteins, we confirmed the previous finding of unchanged plasma TC and TG and increased HDL cholesterol in HCD fed *Cyp8b1*$^{-/-}$ mice (40). The increase in HDL cholesterol may be attributed to the increase in the gene expression of ABCA1 in the livers of *Cyp8b1*$^{-/-}$ mice. Further studies are needed to elucidate the exact mechanism responsible for the increase in HDL cholesterol levels of *Cyp8b1*$^{-/-}$ mice.

Previous observations of reduced intestinal cholesterol absorption in *Cyp8b1*$^{-/-}$ mice (39,40) prompted us to investigate intestinal fat absorption. Interestingly, *Cyp8b1*$^{-/-}$ mice showed diminished intestinal fat absorption. This change in fat absorption correlated with reductions in both adipose depot weights and total body weights in *Cyp8b1*$^{-/-}$ mice. It may be argued that the reduced body weights of the *Cyp8b1*$^{-/-}$ mice may result in improved glucose tolerance and insulin sensitivity, as previously suggested by studies in models of high-fat induced obesity (60). However, similar results in fasting glucose and insulin levels were obtained in body weight matched *Cyp8b1*$^{-/-}$ and control mice (Appendix A), thereby, confirming that the changes in glycemic profile of *Cyp8b1*$^{-/-}$ mice were not due to differences in their body weights.

We hypothesized that reduced fat absorption would affect luminal levels of FFAs, which are potent mediators of incretin release (13). Among the incretin hormones, both GIP and GLP-1 affect β-cell function. While GIP is secreted from the enteroendocrine K-cells in the upper intestine, particularly the duodenum and jejunum, GLP-1 is released from the enteroendocrine L-cells in the distal intestine, in response to nutrient ingestion. The reduction in fat absorption of *Cyp8b1*$^{-/-}$ mice was directly associated with an increase in their luminal FFA content. Luminal FFA levels were most significantly affected in the ileum of *Cyp8b1*$^{-/-}$ mice. These changes suggested that the distal intestinal incretin, GLP-1 is preferentially affected compared to the proximal intestinal incretin GIP. To test this, we assessed levels of GIP and GLP-1 in *Cyp8b1*$^{-/-}$ mice post-oral glucose load. As expected, *Cyp8b1*$^{-/-}$ mice exhibited higher GLP-1 release whereas no significant differences in GIP levels were observed.

We also measured transcript levels of TGR5, the transmembrane bile acid receptor, in the ileum and the colon of our knockout mice and found no change in its expression compared to controls. Thus, increased GLP-1 in the *Cyp8b1*$^{-/-}$ mice may be attributed to increased ileal free fatty acids activating the L-cells and not due to increased TGR5 levels, as previously described (24,25). Further validation of these results such as TGR5 activation assays are necessary to elucidate any possible role of TGR5 in stimulating GLP-1 release in *Cyp8b1*$^{-/-}$ mice.

Furthermore, we observed that improved GLP-1 secretion significantly improved β-cell function in *Cyp8b1*$^{-/-}$ mice. The *Cyp8b1*$^{-/-}$ mice showed significantly increased *in vivo* insulin release in response to glucose as well as increased islet insulin content. Increased GLP-1 levels in *Cyp8b1*$^{-/-}$ mice was associated not only with an improvement in β-cell function but also peripheral insulin sensitivity. Both these effects can be ascribed to GLP-1, a well-known insulin secretagogue that improves β-cell function and can restore insulin sensitivity even in diabetic conditions via the PI-3-kinase pathway (61,62). We also observed that GLP-1 receptor antagonism in *Cyp8b1*$^{-/-}$ mice leads to complete normalization of the improvement in glucose tolerance. This indicates that GLP-1 plays a critical role in shaping the glycemic phenotype of *Cyp8b1*$^{-/-}$ mice.

Recent evidence that murine islets express FXR and TGR5, potent receptors of bile acids (59,63), suggests that the altered peripheral bile acid composition of *Cyp8b1*$^{-/-}$ mice may have a direct and important role in improving islet function. Furthermore, UDCA and its conjugated forms, in particular, have recently been shown to improve glucose metabolism and insulin sensitivity by inducing excretion of hepatic lipids in high fat-fed mice (64). Also, UDCA

treatment has been reported to induce the secretion of GLP-1 in healthy subjects (65). However, acute treatment of control mice with the same bile acid species found in excess in the plasma of *Cyp8b1*$^{-/-}$ mice (α, β and ω MCA as well as UDCA) did not affect glucose tolerance. These results suggest that the bile acid species found in excess do not directly impact β-cell function *in vivo*. We then hypothesized that it is rather the absence of CA or its derivatives that leads to the improvement in the glycemic phenotype of *Cyp8b1*$^{-/-}$ mice.

Our rescue experiments involving CA feeding to *Cyp8b1*$^{-/-}$ mice provide strong evidence that absence of CA results in the improved fat tolerance and consequently improved glucose tolerance in *Cyp8b1*$^{-/-}$ mice. We also investigated the effect of CA feeding on GLP-1 secretion. Interestingly, CA administration abolished the increase in GLP-1 release in *Cyp8b1*$^{-/-}$ mice, suggesting that indeed, the lack of CA is responsible for the improved glycemic control in these mice.

Furthermore, it is also interesting to note that male *Cyp8b1*$^{-/-}$ mice did not show any differences in the lipoprotein profile (Appendix B, Table 4), the fasting glucose and insulin or glucose and insulin tolerance when fed HCD (Appendix C-D). The reason for this sexual dimorphism is not well understood. It has previously been reported that female *Cyp8b1*$^{-/-}$ mice have approximately 35-40% larger bile acid pool size compared to male *Cyp8b1*$^{-/-}$ mice (38), as a consequence of higher *Cyp7a1* output. Additionally it is known that wild-type females have higher cholate compared to their corresponding male littermates (66,67). It is, thus, interesting to speculate that it is this greater deficiency of cholic acid in female *Cyp8b1*$^{-/-}$ mice compared to male *Cyp8b1*$^{-/-}$ mice that may be responsible for these improvements. More studies analyzing

gender-based differences would be useful in determining the reason for improved glucose homeostasis in females alone.

It must also be noted that changes in the bile acid pool of *Cyp8b1*$^{-/-}$ mice are closely recapitulated in germ free, as well as antibiotic treated mice with diminished CA levels and reduction in cholesterol absorption (68,69). Similarly, *Cyp7a1* expression is also up regulated under all three conditions. Interestingly, germ free mice have better glucose tolerance, as well as insulin resistance (70). However, the underlying mechanisms remain unexplored. A recent study directly confirmed the similarity in the bile acid composition of *Cyp8b1*$^{-/-}$ mice and antibiotic treated mice, however, regulation of blood glucose levels was not studied (71). Further studies are needed to understand this relationship between gut microbiota, bile acids, glucose and lipid homeostasis.

Chapter 5: Conclusion

This study is the first to provide evidence that loss of cholic acid production improves glucose metabolism and insulin sensitivity in mice fed a high cholesterol diet. The knockout of *Cyp8b1* also improves β-cell function in these mice. Furthermore, these effects are mediated by increased GLP-1 secretion, possibly in response to increased free fatty acids reaching the ileum (Figure 5.1). The phenotypes observed in *Cyp8b1*$^{-/-}$ mice were lost after administration of either a specific and potent GLP-1 receptor antagonist or cholic acid, suggesting the critical involvement of elevation of GLP-1 and the absence of cholic acid in the observed phenotype.

Given the differences in the bile acid pool in mice and humans, it will be important to determine if similar effects would be observed in humans. Nonetheless, our data strongly demonstrates that the inhibition of *Cyp8b1* has potential therapeutic implications by eliminating 12α- hydroxylated bile acids and thus increasing the level of endogenous GLP-1, in the treatment of T2D.

Figure 5.1

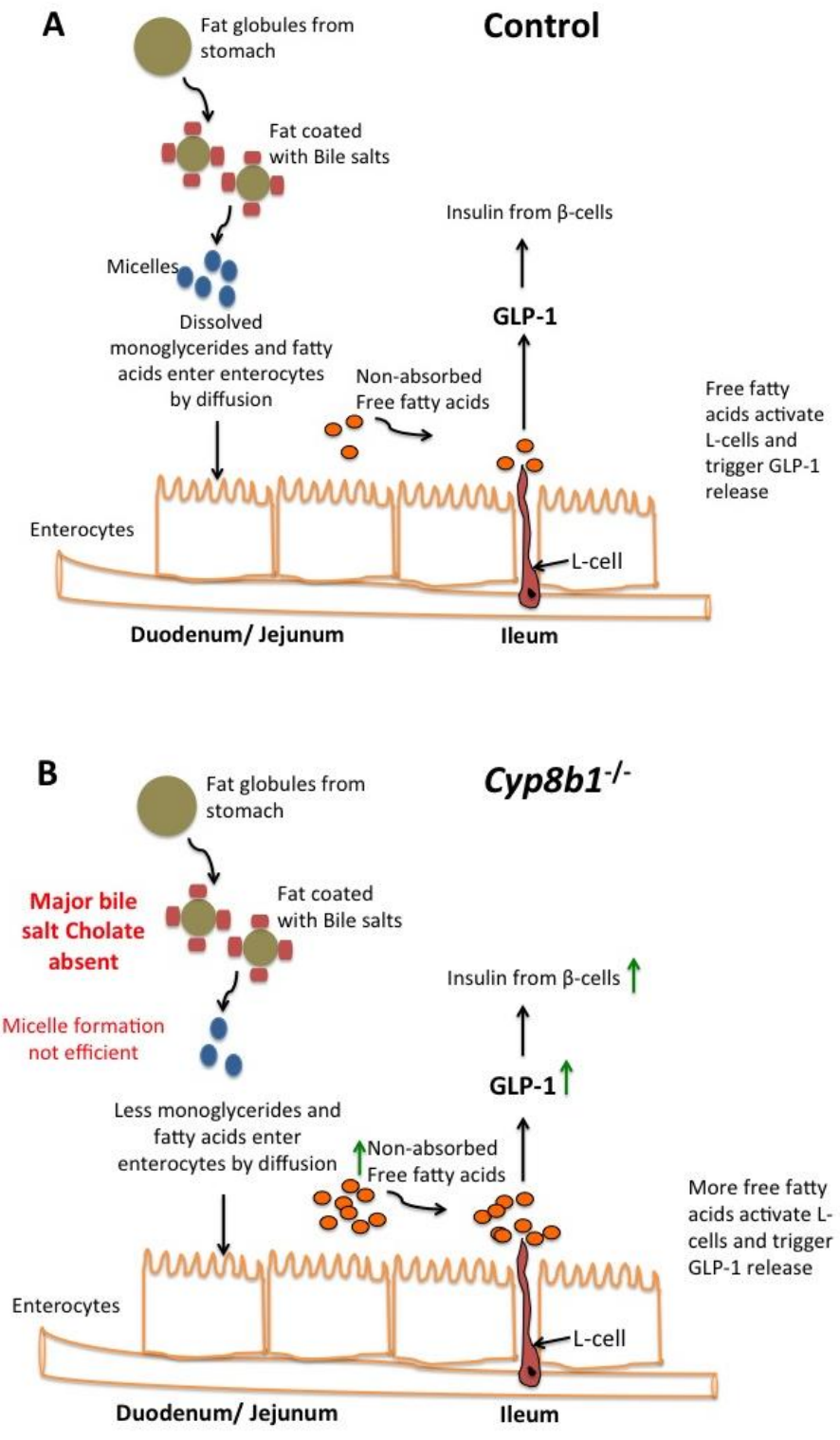
A
Control
Fat globules from stomach
Fat coated with Bile salts
Micelles
Dissolved monoglycerides and fatty acids enter enterocytes by diffusion
Insulin from β-cells
GLP-1
Non-absorbed Free fatty acids
Free fatty acids activate L-cells and trigger GLP-1 release
Enterocytes
L-cell
Duodenum/ Jejunum
Ileum
B
Cyp8b1-/-
Fat globules from stomach
Major bile salt Cholate absent
Fat coated with Bile salts
Micelle formation not efficient
Insulin from β-cells
GLP-1
Less monoglycerides and fatty acids enter enterocytes by diffusion
Non-absorbed Free fatty acids
More free fatty acids activate L-cells and trigger GLP-1 release
Enterocytes
L-cell
Duodenum/ Jejunum
Ileum

Figure 5.1 Mechanism for increased GLP-1 secretion in *Cyp8b1*$^{-/-}$ mice

A. Normal digestive process in control mice. Bile acids are released from the gallbladder on nutrient ingestion and they act on fat from the stomach to produce micelles that facilitate digestion. The monoglycerides and fatty acids diffuse into the enterocytes where they are further processed until they enter the blood stream. The non-absorbed free fatty acids migrate to the terminal ileum where they activate enteroendocrine L-cells to release the incretin, GLP-1. GLP-1 in-turn stimulates the release of insulin from the pancreatic β-cells.

B. *Cyp8b1*$^{-/-}$ mice lack cholic acid and may thus they have defective micellar absorption of fats from the stomach. As a results, more free fatty acids migrate to the terminal ileum, thereby increasing the activity of greater number of enteroendocrine L-cells, resulting in the release of more incretin, GLP-1. Higher GLP-1 release stimulates more insulin release from the pancreatic β-cells.

Chapter 6: Future Perspectives

The number of people affected with T2D worldwide is increasing at an alarming rate. Canada alone has more than 60,000 new cases every year. In the light of this increasing prevalence of T2D, it is essential to develop new therapeutic strategies to combat this disease.

In the current study on *Cyp8b1*$^{-/-}$ mice, we studied the effects of cholic acid inhibition on glucose homeostasis and found a significant improvement in the glycemic control of *Cyp8b1*$^{-/-}$ mice. It will be of interest to determine if therapeutic inhibition of *Cyp8b1* using either anti-sense oligonucleotides (ASO) or other gene silencing methods like short interfering RNA (siRNA), in mouse models of diabetes could also exert similar effects on glucose tolerance, insulin sensitivity and β-cell function. Diet-induced diabetic mice, or commercially available *ob/ob* or *db/db* mice could be used for this therapeutic validation. These studies will enhance the claim that inhibition of *Cyp8b1* could be used as a therapeutic target in the treatment of T2D.

In this study we attempted to determine the effect of increased circulating bile acid in *Cyp8b1*$^{-/-}$ mice by administering these excess species intraperitoneally in wild-type mice. We, however, did not see any direct improvement in glucose tolerance. It would be interesting to check if supplementation of these bile acids in the diet of control mice could have any effect on their islet function. Long term diet supplementation of the excess bile acids (i.e. αMCA, βMCA, ωMCA and UDCA) would enable the wild-type mice to adapt to the changes in transcriptional regulation of bile acid synthesis and change their overall bile acid pool. Thus, shift in the bile

acid pool from cholate to muricholates may also help in improving the glucose homeostasis in mice.

Furthermore, obesity and obesity related T2D are associated with attenuation of afferent and efferent vagus nerve signaling that is implicated in metabolic regulation (72). It is known that nutrient-sensitive vagal afferents respond to fat and carbohydrate ingestion and mediate the release of GLP-1 (14). In *Cyp8b1*$^{-/-}$ mice it is interesting to note that the insulin release peaks at 15 minutes, but GLP-1 secretion is highest at 30 minutes post glucose challenge. It is established that dorsal root ganglia express TGR5 and can thus be stimulated with bile acids. However, if vagal afferents express TGR5 is still not known. It would also be of interest to determine if bile acids have the ability to directly stimulate the vagal afferents via TGR5, and if it leads to increased GLP-1 release. Specific muscarinic and nicotinic acetylcholine receptor inhibitors could be used to elucidate the role of the vagal efferent signaling in *Cyp8b1*$^{-/-}$ mice. Additionally, vagotomies could also be performed to assess the role of vagal control in GLP-1 release in *Cyp8b1*$^{-/-}$ mice.

Cyp8b1 inhibition improves both peripheral insulin sensitivity and glucose tolerance via GLP-1 mediated mechanisms. Since GLP-1 exerts its physiological actions on multiple peripheral tissues, *Cyp8b1*$^{-/-}$ mouse model provides a unique opportunity to study the effects of this gene knockout in different disease models. For instance, brain insulin sensitivity is reduced in Alzheimer disease (AD). Studies have shown that several anti-diabetic drugs can promote neuronal survival and lead to a significant clinical improvement of memory and cognition (73). Also, GLP-1 mimetic drugs have been shown to improve synaptic plasticity and survival via

GSK3β and Akt signaling in mouse model of AD (74). Thus, it would be interesting to study the effect of *Cyp8b1* knockdown in AD mouse models.

Although 172 single nucleotide polymorphisms (SNPs) have been identified for *CYP8B1* (http://www.genecards.org/cgi-bin/carddisp.pl?gene=CYP8B1), no loss-of-function mutations have been determined. Furthermore, none of these SNPs have been associated with any disease phenotype. Thus, it would be of great interest to identify both heterozygous and homozygous carriers of *CYP8B1* mutations in humans. These mutation carriers can then be assessed for their glycemic phenotypes, in order to further validate the development of *CYP8B1* inhibitor therapies to combat diabetes. Sequencing or genotyping of known *CYP8B1* variants will greatly aid in this effort.

Bibliography

1. Aronoff SL, Berkowitz K, Shreiner B. Glucose metabolism and regulation: beyond insulin and glucagon. Diabetes Spectrum. 2004.

2. Leney SE, Tavaré JM. The molecular basis of insulin-stimulated glucose uptake: signalling, trafficking and potential drug targets. J. Endocrinol. 2009Oct.;203(1):1–18.

3. Cohen P, Nimmo HG, Proud CG. How does insulin stimulate glycogen synthesis? Biochem. Soc. Symp. 1978;(43):69–95.

4. Kaneko K, Shirotani T, Araki E, Matsumoto K, Taguchi T, Motoshima H, et al. Insulin inhibits glucagon secretion by the activation of PI3-kinase in In-R1-G9 cells. Diabetes Res. Clin. Pract. 1999May;44(2):83–92.

5. Saltiel AR, Kahn CR. Insulin signalling and the regulation of glucose and lipid metabolism. Nature. 2001Dec.13;414(6865):799–806.

6. Dimitriadis G, Mitrou P, Lambadiari V, Maratou E, Raptis SA. Insulin effects in muscle and adipose tissue. Diabetes Res. Clin. Pract. 2011Aug.;93 Suppl 1:S52–9.

7. Henquin J-C. The dual control of insulin secretion by glucose involves triggering and amplifying pathways in β-cells. Diabetes Res. Clin. Pract. 2011Aug.;93 Suppl 1:S27–31.

8. Straub SG, Sharp GWG. Glucose-stimulated signaling pathways in biphasic insulin secretion. Diabetes Metab. Res. Rev. 2002Nov.;18(6):451–63.

9. Thomas C, Pellicciari R, Pruzanski M, Auwerx J, Schoonjans K. Targeting bile-acid signalling for metabolic diseases. Nat Rev Drug Discov. 2008Aug.;7(8):678–93.

10. Gautier J-F, Choukem S-P, Girard J. Physiology of incretins (GIP and GLP-1) and abnormalities in type 2 diabetes. Diabetes Metab. 2008Feb.;34 Suppl 2:S65–72.

11. Kim W, Egan JM. The role of incretins in glucose homeostasis and diabetes treatment. Pharmacol. Rev. 2008Dec.;60(4):470–512.

12. Baggio LL, Drucker DJ. Biology of incretins: GLP-1 and GIP. Gastroenterology. 2007May;132(6):2131–57.

13. Brubaker PL, Schloos J, Drucker DJ. Regulation of glucagon-like peptide-1 synthesis and secretion in the GLUTag enteroendocrine cell line. Endocrinology. 1998Oct.;139(10):4108–14.

14. Rocca AS, Brubaker PL. Role of the vagus nerve in mediating proximal nutrient-induced

glucagon-like peptide-1 secretion. Endocrinology. 1999Apr.;140(4):1687–94.

15. Muoio DM, Newgard CB. Mechanisms of disease: molecular and metabolic mechanisms of insulin resistance and beta-cell failure in type 2 diabetes. Nat. Rev. Mol. Cell Biol. 2008Mar.;9(3):193–205.

16. Prentki M, Nolan CJ. Islet beta cell failure in type 2 diabetes. J. Clin. Invest. 2006Jul.;116(7):1802–12.

17. Staels B, Fonseca VA. Bile acids and metabolic regulation: mechanisms and clinical responses to bile acid sequestration. Diabetes Care. 2009Nov.;32 Suppl 2:S237–45.

18. Staels B, Kuipers F. Bile acid sequestrants and the treatment of type 2 diabetes mellitus. Drugs. 2007;67(10):1383–92.

19. Stamp D, Jenkins G. An overview of bile-acid synthesis, chemistry and function. … Royal Society of Chemistry. 2008.

20. Chiang JYL. Bile acids: regulation of synthesis. J. Lipid Res. 2009Oct.;50(10):1955–66.

21. Chiang JYL. Bile acid regulation of hepatic physiology: III. Bile acids and nuclear receptors. Am. J. Physiol. Gastrointest. Liver Physiol. 2003Mar.;284(3):G349–56.

22. Porez G, Prawitt J, Gross B, Staels B. Bile acid receptors as targets for the treatment of dyslipidemia and cardiovascular disease. J. Lipid Res. 2012Sep.;53(9):1723–37.

23. Li T, Chiang JYL. Bile Acid signaling in liver metabolism and diseases. J Lipids. 2012;2012:754067.

24. Katsuma S, Hirasawa A, Tsujimoto G. Bile acids promote glucagon-like peptide-1 secretion through TGR5 in a murine enteroendocrine cell line STC-1. Biochem. Biophys. Res. Commun. 2005Apr.1;329(1):386–90.

25. Thomas C, Gioiello A, Noriega L, Strehle A, Oury J, Rizzo G, et al. TGR5-mediated bile acid sensing controls glucose homeostasis. Cell Metab. 2009Sep.;10(3):167–77.

26. Hofmann AF. Bile acid sequestrants improve glycemic control in type 2 diabetes: a proposed mechanism implicating glucagon-like peptide 1 release. Hepatology. 2011May;53(5):1784.

27. Schwarz M, Lund EG, Setchell KD, Kayden HJ, Zerwekh JE, Björkhem I, et al. Disruption of cholesterol 7alpha-hydroxylase gene in mice. II. Bile acid deficiency is overcome by induction of oxysterol 7alpha-hydroxylase. J. Biol. Chem. 1996Jul.26;271(30):18024–31.

28. Ishibashi S, Schwarz M, Frykman PK, Herz J, Russell DW. Disruption of cholesterol 7alpha-hydroxylase gene in mice. I. Postnatal lethality reversed by bile acid and vitamin

supplementation. J. Biol. Chem. 1996Jul.26;271(30):18017–23.

29. Pullinger CR, Eng C, Salen G, Shefer S, Batta AK, Erickson SK, et al. Human cholesterol 7alpha-hydroxylase (CYP7A1) deficiency has a hypercholesterolemic phenotype. J. Clin. Invest. 2002Jul.;110(1):109–17.

30. Abrahamsson A, Gåfvels M, Reihnér E, Björkhem I, Einarsson C, Eggertsen G. Polymorphism in the coding part of the sterol 12alpha-hydroxylase gene does not explain the marked differences in the ratio of cholic acid and chenodeoxycholic acid in human bile. Scand. J. Clin. Lab. Invest. 2005;65(7):595–600.

31. Uchida K, Satoh T, Takase H, Nomura Y, Takasu N, Kurihara H, et al. Altered bile acid metabolism related to atherosclerosis in alloxan diabetic rats. J. Atheroscler. Thromb. 1996;3(1):52–8.

32. Babiker A, Andersson O, Lund E, Xiu RJ, Deeb S, Reshef A, et al. Elimination of cholesterol in macrophages and endothelial cells by the sterol 27-hydroxylase mechanism. Comparison with high density lipoprotein-mediated reverse cholesterol transport. J. Biol. Chem. 1997Oct.17;272(42):26253–61.

33. Pandak WM, Ren S, Marques D, Hall E, Redford K, Mallonee D, et al. Transport of cholesterol into mitochondria is rate-limiting for bile acid synthesis via the alternative pathway in primary rat hepatocytes. J. Biol. Chem. 2002Dec.13;277(50):48158–64.

34. Botham KM, Boyd GS. The metabolism of chenodeoxycholic acid to beta-muricholic acid in rat liver. Eur. J. Biochem. 1983Jul.15;134(1):191–6.

35. Ishida H, Noshiro M, Okuda K, Coon MJ. Purification and characterization of 7 alpha-hydroxy-4-cholesten-3-one 12 alpha-hydroxylase. J. Biol. Chem. 1992Oct.25;267(30):21319–23.

36. Gåfvels M, Olin M, Chowdhary BP, Raudsepp T, Andersson U, Persson B, et al. Structure and chromosomal assignment of the sterol 12alpha-hydroxylase gene (CYP8B1) in human and mouse: eukaryotic cytochrome P-450 gene devoid of introns. Genomics. 1999Mar.1;56(2):184–96.

37. Norlin M, Wikvall K. Enzymes in the conversion of cholesterol into bile acids. Curr. Mol. Med. 2007Mar.;7(2):199–218.

38. Li-Hawkins J, Gåfvels M, Olin M, Lund EG, Andersson U, Schuster G, et al. Cholic acid mediates negative feedback regulation of bile acid synthesis in mice. J. Clin. Invest. 2002Oct.;110(8):1191–200.

39. Murphy C, Parini P, Wang J, Björkhem I, Eggertsen G, Gåfvels M. Cholic acid as key regulator of cholesterol synthesis, intestinal absorption and hepatic storage in mice. Biochim. Biophys. Acta. 2005Aug.15;1735(3):167–75.

40. Wang J, Einarsson C, Murphy C, Parini P, Björkhem I, Gåfvels M, et al. Studies on LXR- and FXR-mediated effects on cholesterol homeostasis in normal and cholic acid-depleted mice. J. Lipid Res. 2006Feb.;47(2):421–30.

41. Slätis K, Gåfvels M, Kannisto K, Ovchinnikova O, Paulsson-Berne G, Parini P, et al. Abolished synthesis of cholic acid reduces atherosclerotic development in apolipoprotein E knockout mice. J. Lipid Res. 2010Nov.;51(11):3289–98.

42. Wang J, Gåfvels M, Rudling M, Murphy C, Björkhem I, Einarsson C, et al. Critical role of cholic acid for development of hypercholesterolemia and gallstones in diabetic mice. Biochem. Biophys. Res. Commun. 2006Apr.21;342(4):1382–8.

43. Wang J, Greene S, Eriksson LC, Rozell B, Reihnér E, Einarsson C, et al. Human sterol 12a-hydroxylase (CYP8B1) is mainly expressed in hepatocytes in a homogenous pattern. Histochem. Cell Biol. 2005Jun.;123(4-5):441–6.

44. Li T, Owsley E, Matozel M, Hsu P, Novak CM, Chiang JYL. Transgenic expression of cholesterol 7alpha-hydroxylase in the liver prevents high-fat diet-induced obesity and insulin resistance in mice. Hepatology. 2010Aug.;52(2):678–90.

45. Keane MH, Overmars H, Wikander TM, Ferdinandusse S, Duran M, Wanders RJA, et al. Bile acid treatment alters hepatic disease and bile acid transport in peroxisome-deficient PEX2 Zellweger mice. Hepatology. 2007Apr.;45(4):982–97.

46. Folch J, Lees M, Sloane Stanley GH. A simple method for the isolation and purification of total lipides from animal tissues. J. Biol. Chem. 1957May;226(1):497–509.

47. Hardy AB, Wijesekara N, Genkin I, Prentice KJ, Bhattacharjee A, Kong D, et al. Effects of high-fat diet feeding on Znt8-null mice: differences between β-cell and global knockout of Znt8. Am. J. Physiol. Endocrinol. Metab. 2012May15;302(9):E1084–96.

48. Kruit JK, Wijesekara N, Fox JEM, Dai X-Q, Brunham LR, Searle GJ, et al. Islet cholesterol accumulation due to loss of ABCA1 leads to impaired exocytosis of insulin granules. Diabetes. 2011Dec.;60(12):3186–96.

49. Hulzebos CV, Renfurm L, Bandsma RH, Verkade HJ, Boer T, Boverhof R, et al. Measurement of parameters of cholic acid kinetics in plasma using a microscale stable isotope dilution technique: application to rodents and humans. J. Lipid Res. 2001Nov.;42(11):1923–9.

50. Trauner M, Claudel T, Fickert P, Moustafa T, Wagner M. Bile acids as regulators of hepatic lipid and glucose metabolism. Dig Dis. 2010;28(1):220–4.

51. Nauck M, Stöckmann F, Ebert R, Creutzfeldt W. Reduced incretin effect in type 2 (non-insulin-dependent) diabetes. Diabetologia. 1986Jan.;29(1):46–52.

52. Haeusler RA, Astiarraga B, Camastra S, Accili D, Ferrannini E. Human Insulin Resistance

is Associated with Increased Plasma Levels of 12α-hydroxylated Bile Acids. Diabetes. 2013Jul.24.

53. Hirasawa A, Tsumaya K, Awaji T, Katsuma S, Adachi T, Yamada M, et al. Free fatty acids regulate gut incretin glucagon-like peptide-1 secretion through GPR120. Nat. Med. 2005Jan.;11(1):90–4.

54. Fehmann HC, Habener JF. Insulinotropic hormone glucagon-like peptide-I(7-37) stimulation of proinsulin gene expression and proinsulin biosynthesis in insulinoma beta TC-1 cells. Endocrinology. 1992Jan.;130(1):159–66.

55. Xu G, Stoffers DA, Habener JF, Bonner-Weir S. Exendin-4 stimulates both beta-cell replication and neogenesis, resulting in increased beta-cell mass and improved glucose tolerance in diabetic rats. Diabetes. 1999Dec.;48(12):2270–6.

56. Perfetti R, Zhou J, Doyle ME, Egan JM. Glucagon-like peptide-1 induces cell proliferation and pancreatic-duodenum homeobox-1 expression and increases endocrine cell mass in the pancreas of old, glucose-intolerant rats. Endocrinology. 2000Dec.;141(12):4600–5.

57. Juang J-H, Kuo C-H, Wu C-H, Juang C. Exendin-4 treatment expands graft beta-cell mass in diabetic mice transplanted with a marginal number of fresh islets. Cell Transplant. 2008;17(6):641–7.

58. Sathananthan M, Farrugia LP, Miles JM, Piccinini F, Dalla Man C, Zinsmeister AR, et al. Direct effects of exendin-(9,39) and GLP-1-(9,36)amide on insulin action, β-cell function, and glucose metabolism in nondiabetic subjects. Diabetes. 2013Aug.;62(8):2752–6.

59. Kumar DP, Rajagopal S, Mahavadi S, Mirshahi F, Grider JR, Murthy KS, et al. Activation of transmembrane bile acid receptor TGR5 stimulates insulin secretion in pancreatic β cells. Biochem. Biophys. Res. Commun. 2012Oct.26;427(3):600–5.

60. Surwit RS, Kuhn CM, Cochrane C, McCubbin JA, Feinglos MN. Diet-induced type II diabetes in C57BL/6J mice. Diabetes. 1988Sep.;37(9):1163–7.

61. Idris I, Patiag D, Gray S, Donnelly R. Exendin-4 increases insulin sensitivity via a PI-3-kinase-dependent mechanism: contrasting effects of GLP-1. Biochem. Pharmacol. 2002Mar.1;63(5):993–6.

62. Zander M, Madsbad S, Madsen JL, Holst JJ. Effect of 6-week course of glucagon-like peptide 1 on glycaemic control, insulin sensitivity, and beta-cell function in type 2 diabetes: a parallel-group study. Lancet. 2002Mar.9;359(9309):824–30.

63. Düfer M, Hörth K, Wagner R, Schittenhelm B, Prowald S, Wagner TFJ, et al. Bile acids acutely stimulate insulin secretion of mouse β-cells via farnesoid X receptor activation and K(ATP) channel inhibition. Diabetes. 2012Jun.;61(6):1479–89.

64. Tsuchida T, Shiraishi M, Ohta T, Sakai K, Ishii S. Ursodeoxycholic acid improves insulin sensitivity and hepatic steatosis by inducing the excretion of hepatic lipids in high-fat diet-fed KK-Ay mice. Metab. Clin. Exp. 2012Jul.;61(7):944–53.

65. Murakami M, Une N, Nishizawa M, Suzuki S, Ito H, Horiuchi T. Incretin secretion stimulated by ursodeoxycholic acid in healthy subjects. Springerplus. 2013Dec.;2(1):20.

66. Schwarz M, Russell DW, Dietschy JM, Turley SD. Alternate pathways of bile acid synthesis in the cholesterol 7alpha-hydroxylase knockout mouse are not upregulated by either cholesterol or cholestyramine feeding. J. Lipid Res. 2001Oct.;42(10):1594–603.

67. Turley SD, Schwarz M, Spady DK, Dietschy JM. Gender-related differences in bile acid and sterol metabolism in outbred CD-1 mice fed low- and high-cholesterol diets. Hepatology. 1998Oct.;28(4):1088–94.

68. Steiner A, Howard E, Akgun S. Effect of antibiotics on the serum cholesterol concentration of patients with astherosclerosis. Circulation. 1961Oct.;24:729–35.

69. Sayin SI, Wahlström A, Felin J, Jäntti S, Marschall H-U, Bamberg K, et al. Gut microbiota regulates bile acid metabolism by reducing the levels of tauro-beta-muricholic acid, a naturally occurring FXR antagonist. Cell Metab. 2013Feb.5;17(2):225–35.

70. Caesar R, Reigstad CS, Bäckhed HK, Reinhardt C, Ketonen M, Lundén GÖ, et al. Gut-derived lipopolysaccharide augments adipose macrophage accumulation but is not essential for impaired glucose or insulin tolerance in mice. Gut. 2012Dec.;61(12):1701–7.

71. Hu X, Bonde Y, Eggertsen G, Rudling M. Muricholic bile acids are potent regulators of bile acid synthesis via a positive feedback mechanism. J. Intern. Med. 2013Sep.30.

72. Pavlov VA, Tracey KJ. The vagus nerve and the inflammatory reflex--linking immunity and metabolism. Nat Rev Endocrinol. 2012Dec.;8(12):743–54.

73. Patrone C, Eriksson O, Lindholm D. Diabetes drugs and neurological disorders: new views and therapeutic possibilities. Lancet Diabetes Endocrinol. 2014Mar.;2(3):256–62.

74. Ma T, Du X, Pick JE, Sui G, Brownlee M, Klann E. Glucagon-like peptide-1 cleavage product GLP-1(9-36) amide rescues synaptic plasticity and memory deficits in Alzheimer's disease model mice. J. Neurosci. 2012Oct.3;32(40):13701–8.

Appendix A Improved glycemic control in body weight matched *Cyp8b1*$^{-/-}$ mice

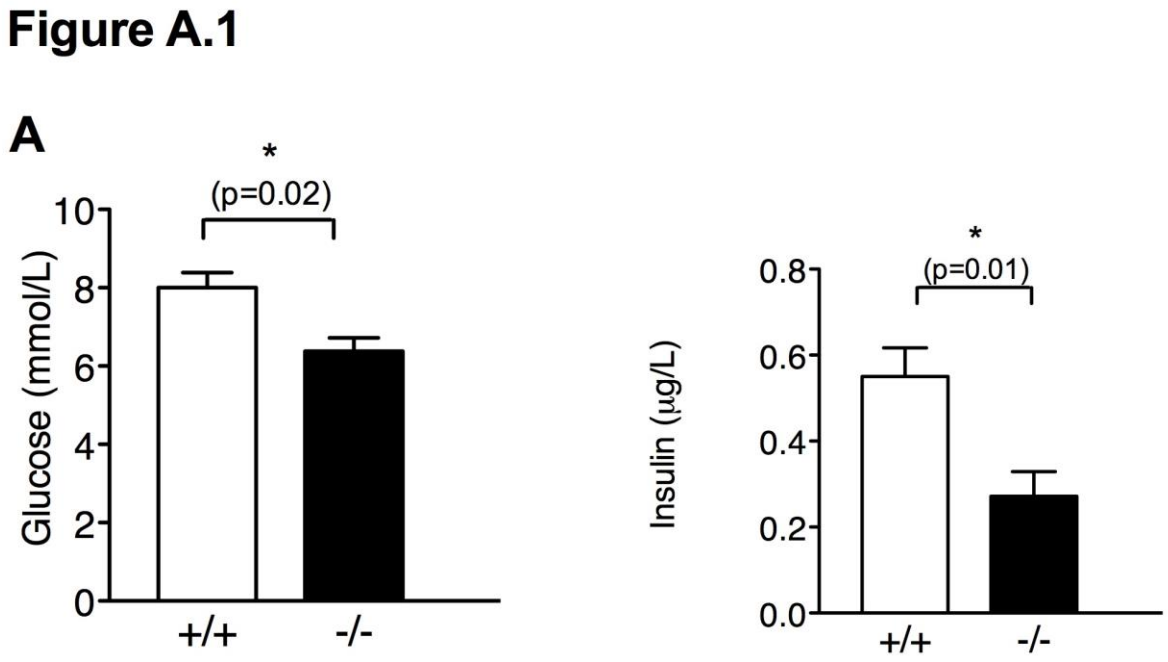

Appendix Figure A.1 Body weight matching causes no change in glycemic profile of *Cyp8b1*$^{-/-}$ mice

A. Fasting glucose and fasting insulin for body weight matched control (+/+) and *Cyp8b1*$^{-/-}$ (-/-) mice on 0.5% cholesterol diet (HCD). Mice were fasted for 4h before blood was drawn. Data expressed as mean± SEM; n=4; *$p<0.05$ by Student's t-test.

Appendix B Improved glycemic control in 6-month-old female *Cyp8b1*$^{-/-}$ mice

Figure B.1

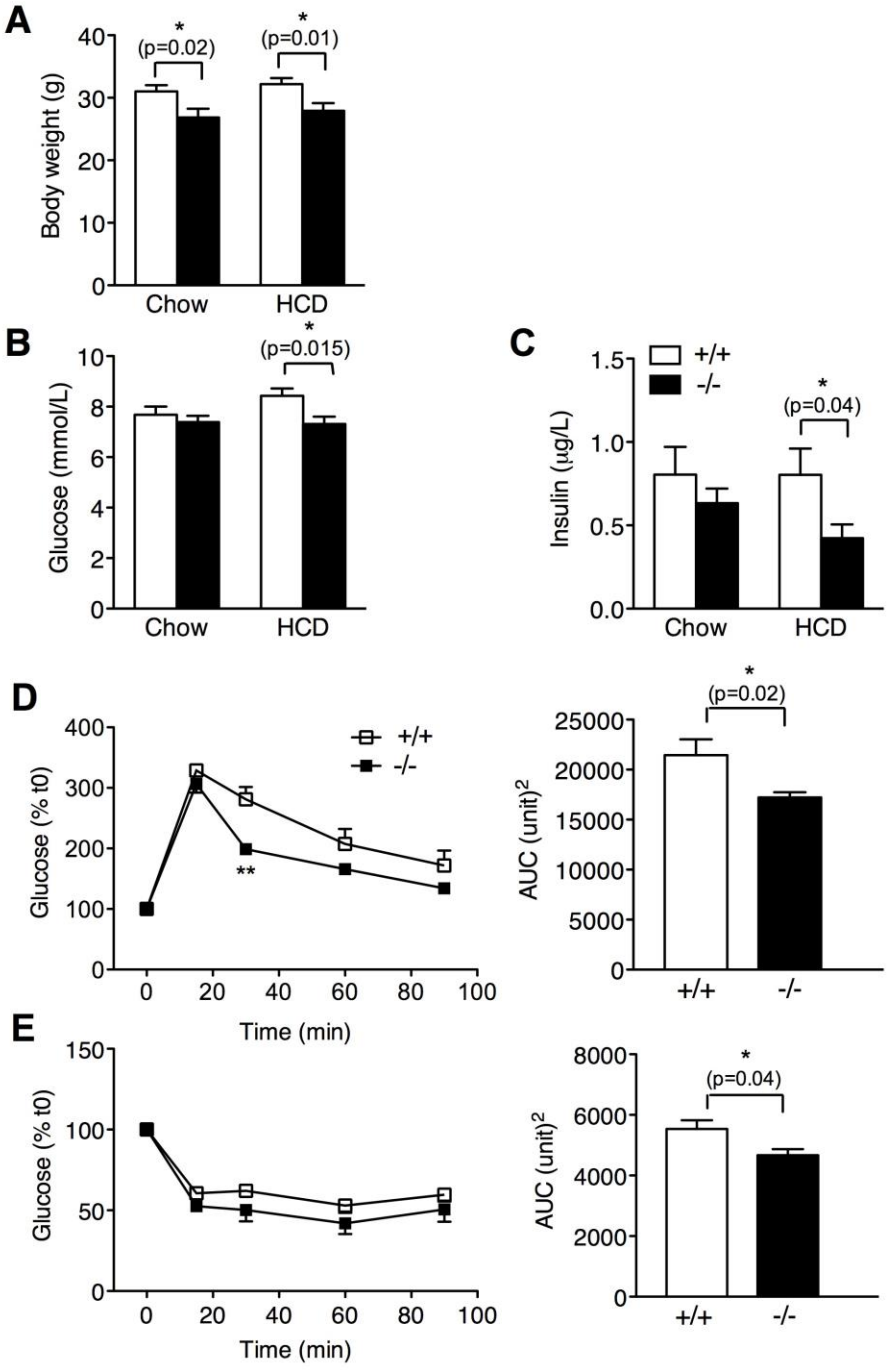

Appendix Figure B.1 Improved glycemic profile of 6-month-old female *Cyp8b1*$^{-/-}$ mice

A. Body weight was measured for control (+/+) and *Cyp8b1*$^{-/-}$ (-/-) mice on chow and 0.5% cholesterol diet (HCD). Data expressed as mean± SEM; n=5-11; *p<0.05 by Student's t-test.

B. Baseline glucose was measured after 4h fasting for control (+/+) and *Cyp8b1*$^{-/-}$ (-/-) mice fed regular chow and HCD. Data expressed as mean± SEM; n=5-11; *p<0.05 by Student's t-test.

C. Baseline insulin was measured after 4h fasting for control (+/+) and *Cyp8b1*$^{-/-}$ (-/-) mice fed regular chow and HCD. Data expressed as mean± SEM; n=5-9; *p<0.05 by Student's t-test.

D. Intraperitoneal glucose tolerance test (IPGTT) along with AUC from control (+/+) and *Cyp8b1*$^{-/-}$ (-/-) mice fed HCD for 4 weeks. Data are shown as mean ± SEM; n=6; **p<0.01 by two-way ANOVA followed by the Bonferroni post-hoc test, AUC *p=0.02 by Student's t-test.

E. Intraperitoneal insulin tolerance test (IPITT) along with AUC from control (+/+) and *Cyp8b1*$^{-/-}$ (-/-) mice fed HCD for 4 weeks. Data are shown as mean ± SEM; n=5-7; *p=0.04 by Student's t-test for AUC.

Appendix C Plasma lipoprotein profile of male *Cyp8b1*$^{-/-}$ mice

		3 months			6 months		
		Control	***Cyp8b1*$^{-/-}$**	**p value**	**Control**	***Cyp8b1*$^{-/-}$**	**p value**
Chow	TC (mM)	3.02±0.21	2.94±0.19	0.79	3.14±0.18	2.94±0.12	0.36
	HDLc (mM)	2.76±0.22	3.37±0.59	0.37	2.54±0.18	2.14±0.48	0.40
	TG (mg/mL)	1.23±0.20	1.04±0.10	0.53	1.07±0.14	0.93±0.07	0.41
HCD	TC (mM)	3.51±0.41	3.62±0.19	0.73	3.84±0.27	3.98±0.27	0.70
	HDLc (mM)	2.91±0.55	3.53±0.08	0.77	2.81±0.38	3.75±0.29	0.08
	TG (mg/mL)	0.68±0.05	0.62±0.02	0.42	0.70±0.02	0.65±0.03	0.24

Table 4 Plasma lipoprotein profile of male control and *Cyp8b1*$^{-/-}$ mice

Fasting plasma lipoproteins including total cholesterol (TC), HDL cholesterol (HDLc) and triglycerides (TG) were quantified from both male control and *Cyp8b1*$^{-/-}$ mice. n= 5-11. Data expressed as mean±SEM.

Appendix D No change in glycemic profile of 3- and 6-month-old male *Cyp8b1*$^{-/-}$ mice

Figure D.1

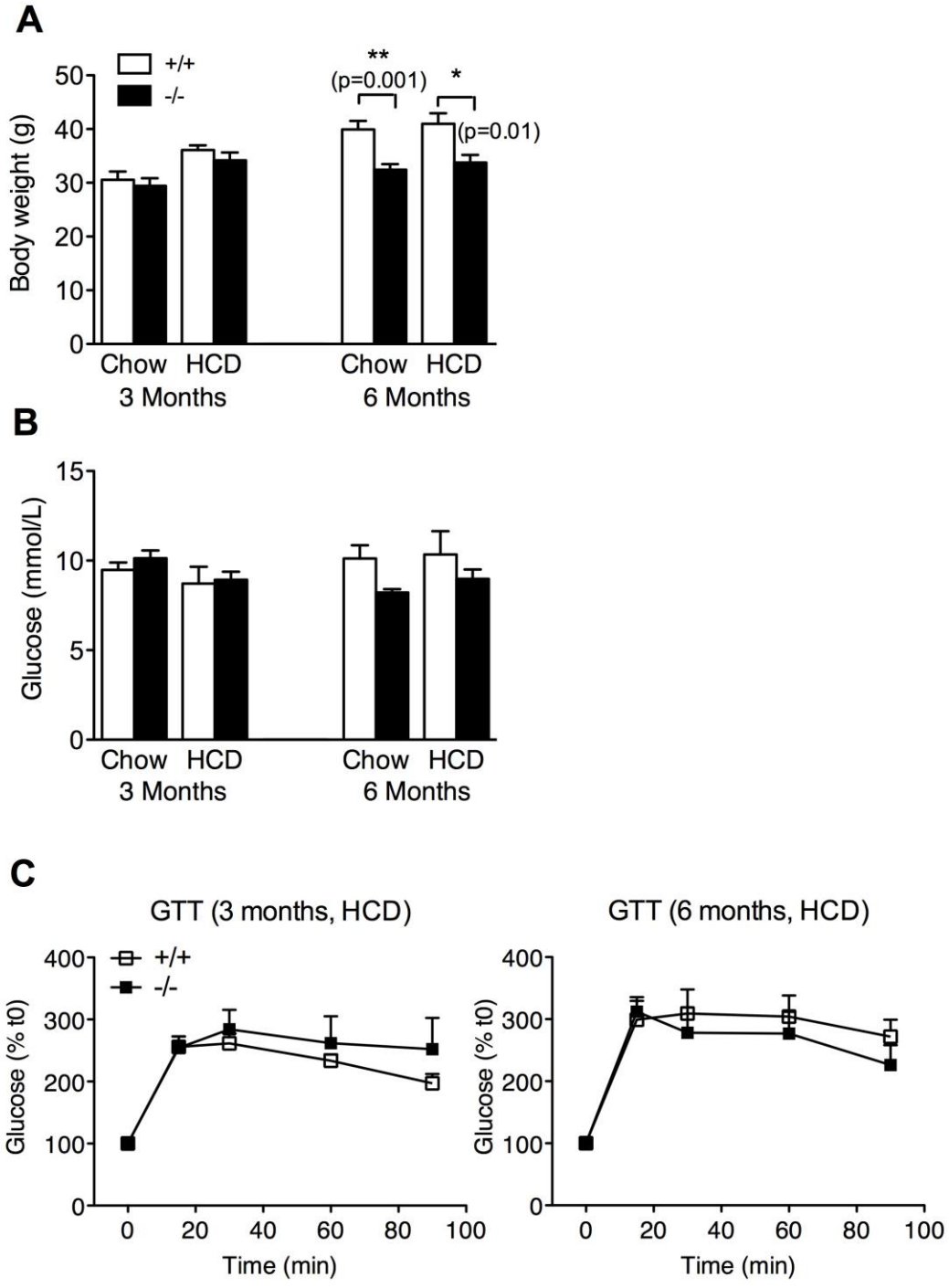

Appendix Figure D.1 No change in glucose parameters of 3 and 6-month-old male *Cyp8b1*$^{-/-}$ mice

A. Body weight was measured for male control (+/+) and *Cyp8b1*$^{-/-}$(-/-) mice fed regular chow and 0.5% cholesterol diet (HCD) for 4 weeks. Data expressed as mean± SEM; n=5-11; **p<0.01, p<0.05 by Student's t-test.
B. Baseline glucose was measured after 4h fasting for male control (+/+) and *Cyp8b1*$^{-/-}$ (-/-) mice fed regular chow and HCD for 4 weeks. Data expressed as mean± SEM; n=5-11; *p<0.05 by Student's t-test.
C. Intraperitoneal glucose tolerance test (IPGTT) from both 3 and 6 months male control (+/+) and *Cyp8b1*$^{-/-}$ (-/-) mice fed HCD for 4 weeks. Data are shown as mean ± SEM n=6.

Figure D.2

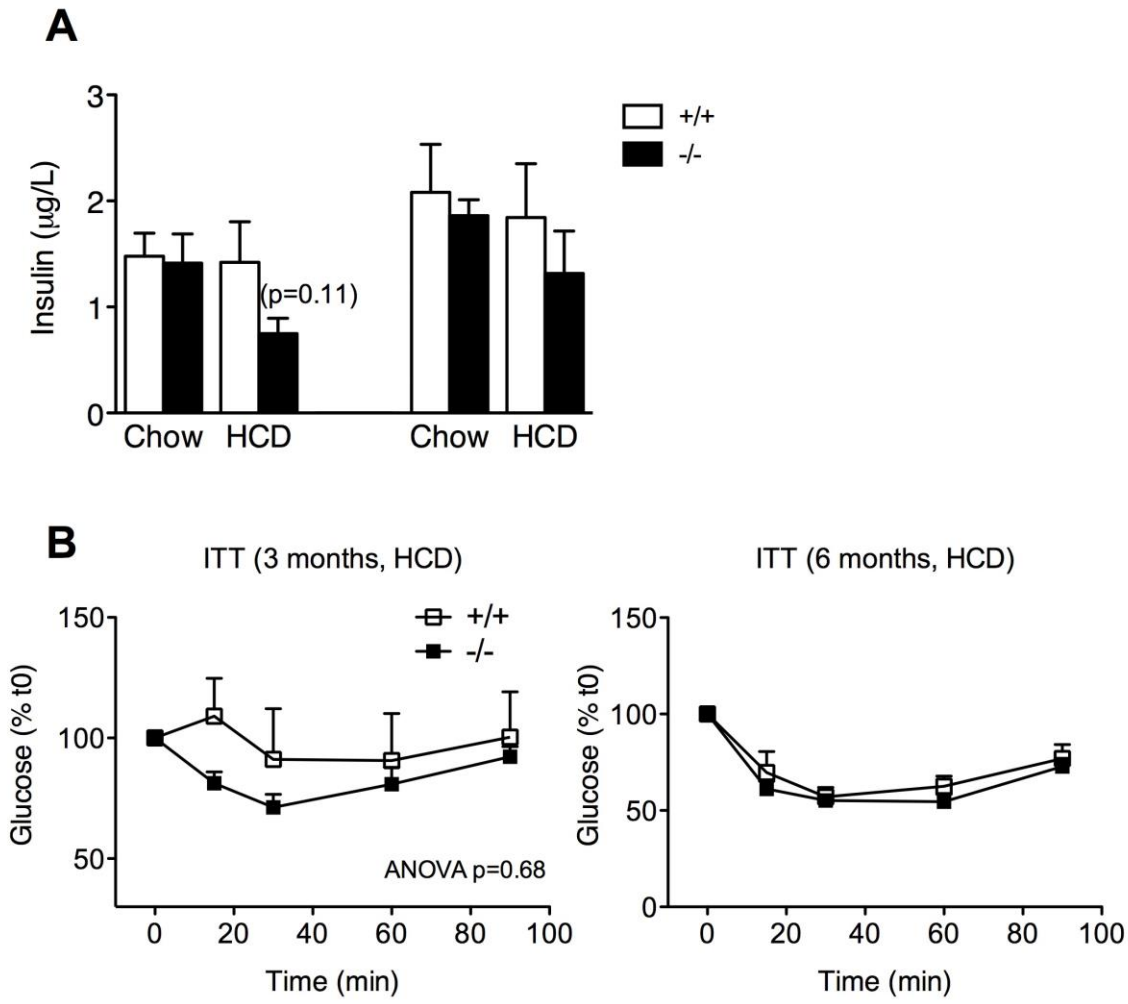

Appendix Figure D.2 No change in insulin parameters of 3- and 6-month-old male *Cyp8b1*$^{-/-}$ mice

- **A.** Baseline insulin was measured after 4h fasting for male control (+/+) and *Cyp8b1*$^{-/-}$ (-/-) mice fed regular chow and 0.5% cholesterol diet (HCD) for 4 weeks. Data expressed as mean± SEM; n=5-11.
- **B.** Intraperitoneal insulin tolerance test (IPITT) from both 3 and 6 month old male control (+/+) and *Cyp8b1*$^{-/-}$ (-/-) mice fed HCD for 4 weeks. Data are shown as mean ± SEM, n=5-7.

Appendix E Circulating bile acid profile of male *Cyp8b1*$^{-/-}$ mice

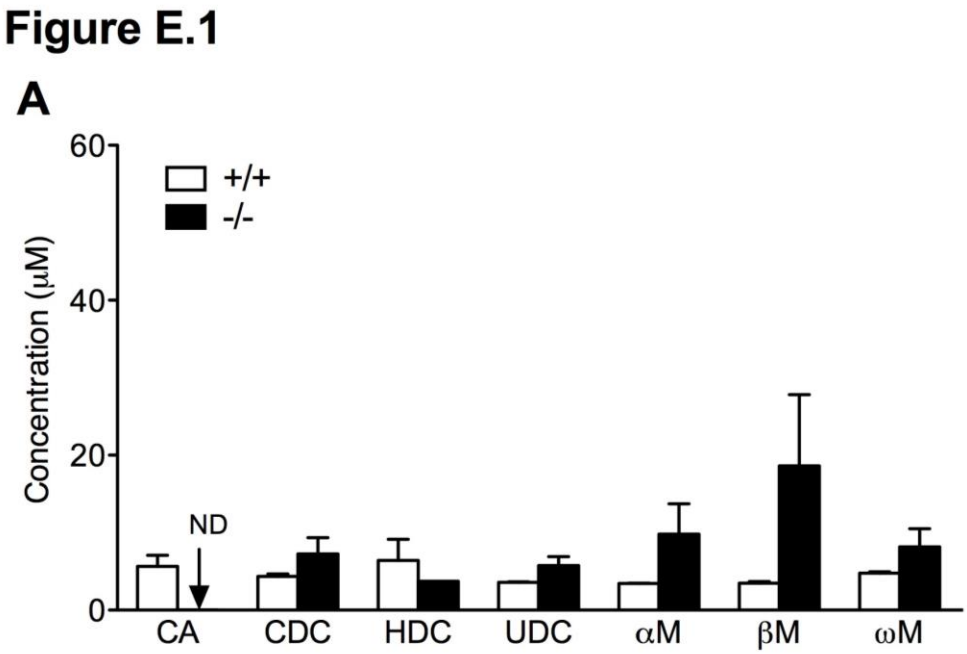

Appendix Figure E.1 Circulating bile acid pool of male *Cyp8b1*$^{-/-}$ mice

A. Plasma bile acid pool in male control (+/+) and *Cyp8b1*$^{-/-}$ (-/-) mice where CA-cholic acid, CDC- chenodeoxycholic acid, HDC-hyodeoxycholic acid, UDC-ursodeoxycholic acid, α/β/ω MCA- α/β/ω muricholic acid. ND- not detectable, Data shown as mean± SEM; n=5.